

SIMULATION OF FORELAND BASIN
STRATIGRAPHY USING A DIFFUSION MODEL OF
MOUNTAIN BELT UPLIFT AND EROSION: AN
EXAMPLE FROM THE CENTRAL ALPS,
SWITZERLAND

H.D. Sinclair¹

Department of Earth Sciences, Oxford University, Oxford,
England.

B.J. Coakley

Lamont-Doherty Geological Observatory and Department
of Geological Sciences, Columbia University, Palisades
New York.

P.A. Allen and A.B. Watts

Department of Earth Sciences, Oxford University, Oxford,
England

Abstract. Foreland basin stratigraphy can be considered as the result of three interacting processes: thrust deformation, which builds the tectonic load, sedimentary and erosional processes which redistribute that load, and the flexural response of the lithosphere. The resultant stratigraphy of foreland basins is commonly composed of a small number of shallowing and coarsening upward cycles bounded by regional unconformities. To understand the development of these unconformities, we present a simple model of these three processes, coupling an evolving thrust wedge on a linear elastic plate with erosion and sedimentation defined by the diffusion equation applied to topography. Our model demonstrates the development of regional unconformities without recourse to either eustasy or complex viscoelastic models for the continental lithosphere. The model describes the thrust wedge-foreland basin system in terms of four parameters: (1) the effective elastic thickness of the foreland plate (T_e), (2) the sediment transport coefficient (K), (3) the thrust wedge advance rate, (4) the surface slope of the thrust wedge. The model is applied to the Oligocene-Miocene North Alpine Foreland Basin (NAFB) of eastern Switzerland. The stratigraphy of the NAFB can be simplified into two large-scale shallowing upward cycles separated by an unconformity at the base of the Burdigalian (22 Ma). Geological information is taken from the NAFB to estimate suitable values for the parameters listed above. Assuming a linear elastic lithospheric rheology, the T_e value is estimated at 10 ± 5

km from decompacted sediment columns. Data to constrain the sequential development of the thrust wedge come from structural geology. The early stages (40-24 Ma) of compression involved a relatively low-angle thrust wedge with an advance rate of approximately 2-4 mm/yr. At about 24 Ma the wedge advance slowed down and thickened by underplating crystalline basement of the foreland plate. The value for the transport coefficient has been estimated from previous studies. Prior to attempting to simulate the broad-scale geometry of the NAFB the role of each parameter was assessed individually. The values for T_e and K are held constant throughout the simulation of the NAFB at 7.5 km and 500 m²/yr, respectively. The geometry of the base Burdigalian unconformity is reproduced by variations in the parameters describing the thrust wedge. The surface slope angle of the wedge is increased from 2.5° to 4° over 0.2 m.y., and the rate of thrust advance is decreased from 2 mm/yr to 0.2 mm/yr, during the thickening event between 24 and 23.8 Ma. The rejuvenation of the internal parts of the thrust load causes backtilting of the foreland basin sediments and, after a time lag, erosion of the distal stratigraphy over the forebulge, so simulating the base Burdigalian unconformity.

INTRODUCTION

Foreland basins are the flexural depressions that develop in front of migrating thrust loads in orogenic belts. The convergence of the orogenic thrust wedge and the foreland plate can be considered in simple mechanical terms as a vertical load translating over a flexing plate. Erosion from the thrust wedge and sedimentation in the flexural depression act to redistribute the effective load, modifying the geometry of the basin. The stratigraphy within the basin preserves a record of the development of the thrust wedge-foreland basin system through time. This study explores the possible controls on foreland

¹Now at Department of Geological Sciences, Science Laboratories, Durham, England.

basin stratigraphy by the evolution of an eroding thrust wedge.

Qualitative understanding of the link between the thrust wedge and its associated foreland basin was first recognized by Price [1973] for the thin-skinned fold and thrust belt of the Southern Canadian Rockies. Price suggested that through this link one might expect to read the history of the thrust wedge in the stratigraphy of the basin.

The concept of lithospheric flexure dates from gravimetric measurements in the oceans [Vening-Meinesz, 1941]. Studies of the oceanic lithosphere at oceanic islands and seamounts [Watts and Cochran, 1974] and at the sites of plate subduction at deep-sea trenches [Watts and Talwani, 1974] indicate that the oceanic lithosphere can be treated as a linear elastic solid whose long-term ($>10^6$ years) strength is dependent on its thermal age [Watts, 1978]. Whether the continental lithosphere can be treated as a linear elastic solid or whether it exhibits some form of stress relaxation on geological time scales is a subject of controversy. Both models have been applied to foreland basins [Jordan, 1981; Quinlan and Beaumont, 1984]. For a linear elastic model to be valid, stress relaxation following loading must be on a short time scale ($<10^5$ - 10^6 m.y.) relative to the time it takes for the basin to fill. If the plate is initially elastic, but then shows significant stress relaxation on long time scales (>20 - 30 m.y.), then viscoelastic relaxation should be observable in the basin stratigraphy.

If we consider a static load on a linear elastic plate, the geometry of the deflection will remain unchanged through time. In contrast, a viscoelastic plate model predicts a narrowing and deepening of the deflection with time. Therefore the stratigraphies of foreland basins should provide an ideal data base for the testing of these rheologies. If we consider the simple case of a stationary load on an elastic plate, with successive stratigraphic units filling the basin to a horizontal datum level, each unit should overstep the previous unit, overlapping the forebulge. On a viscoelastic lithosphere, narrowing of the basin causes each unit to be more confined than the previous unit. This results in stratigraphic offlap, with basin deepening next to the thrust front. However, a conclusive test of these two rheologies is complicated by three processes: (1) motion of the load relative to the plate, (2) changes in the shape and magnitude of the load, (3) erosion and sedimentation, which has the effect of redistributing the load from the thrust wedge to the foreland basin. The steady advance of the load and redistribution of the load by erosion and sedimentation both result in steady stratigraphic onlap onto the foreland. Rejuvenation of the load in the internal parts of the thrust wedge by processes such as out-of-sequence thrusting, backthrusting, and underplating can have the opposite effect, dragging the forebulge towards the mountain belt and forming a regional unconformity in the outer portion of the basin.

The presence of unconformities in foreland basin stratigraphy, apparently correlating with periods of tectonic quiescence and basin deepening close to the thrust front, is the primary evidence for the documentation of viscoelastic relaxation of the lithosphere [Beaumont, 1978; Quinlan and Beaumont, 1984; Willets et al., 1985; Tankard, 1986; Beaumont et al., 1988]. The aims of this paper are to demonstrate that unconformities within

foreland basin stratigraphy can be developed on a purely elastic lithosphere by simply changing the spatial distribution of the load. Sequential structural restoration of the thrust wedge is required to understand how the load has evolved over time. We simulate the stratigraphy of a well-documented foreland basin, the Oligocene-Miocene North Alpine Foreland Basin (NAFB) (Figure 1) subject to the constraint provided by this restoration, and by incorporating the effects of erosion and sediment deposition. The stratigraphy of the NAFB is divided into two large scale shallowing upward cycles separated by an unconformity (Figure 2). This unconformity is dated as base Burdigalian (early Miocene) and is correlated with the underplating of the crystalline basement of the foreland plate onto the base of the thrust wedge [Berger, 1985; Naef et al., 1985; Pfiffner, 1986]. This major event in the development of the Alpine thrust wedge changed the locus of loading, causing uplift of the external parts of the NAFB, so cutting the unconformity. This relationship between loading and peripheral uplift will be documented using radiometric, structural, and stratigraphic data and reproduced through computer modeling.

We cannot ignore that unconformities will result from eustatic fluctuations [Vail et al., 1977; Haq et al., 1987], but the aims of this work are to propose an alternative to either eustasy or stress relaxation in the lithosphere in the formation of unconformities in foreland basins. Consequently, we do not consider this to be an unique solution. Our model is intended to lead to a better physical insight into the possible controls on foreland basin stratigraphy.

DESCRIPTION OF THE MODEL

Foreland basin stratigraphy results from the interaction of an applied force system (load) and the strength of the flexed plate, linked by erosion and sediment deposition. It is essential to study the variation

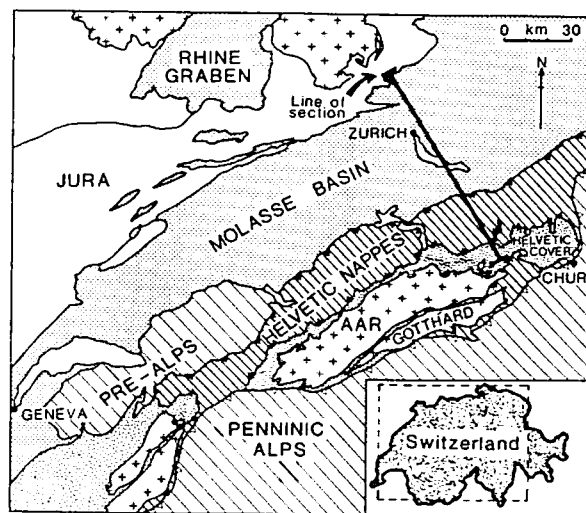


Fig. 1. Simple tectonic map of northern Swiss Alps. Section of study through the North Alpine Foreland Basin (NAFB) is located.

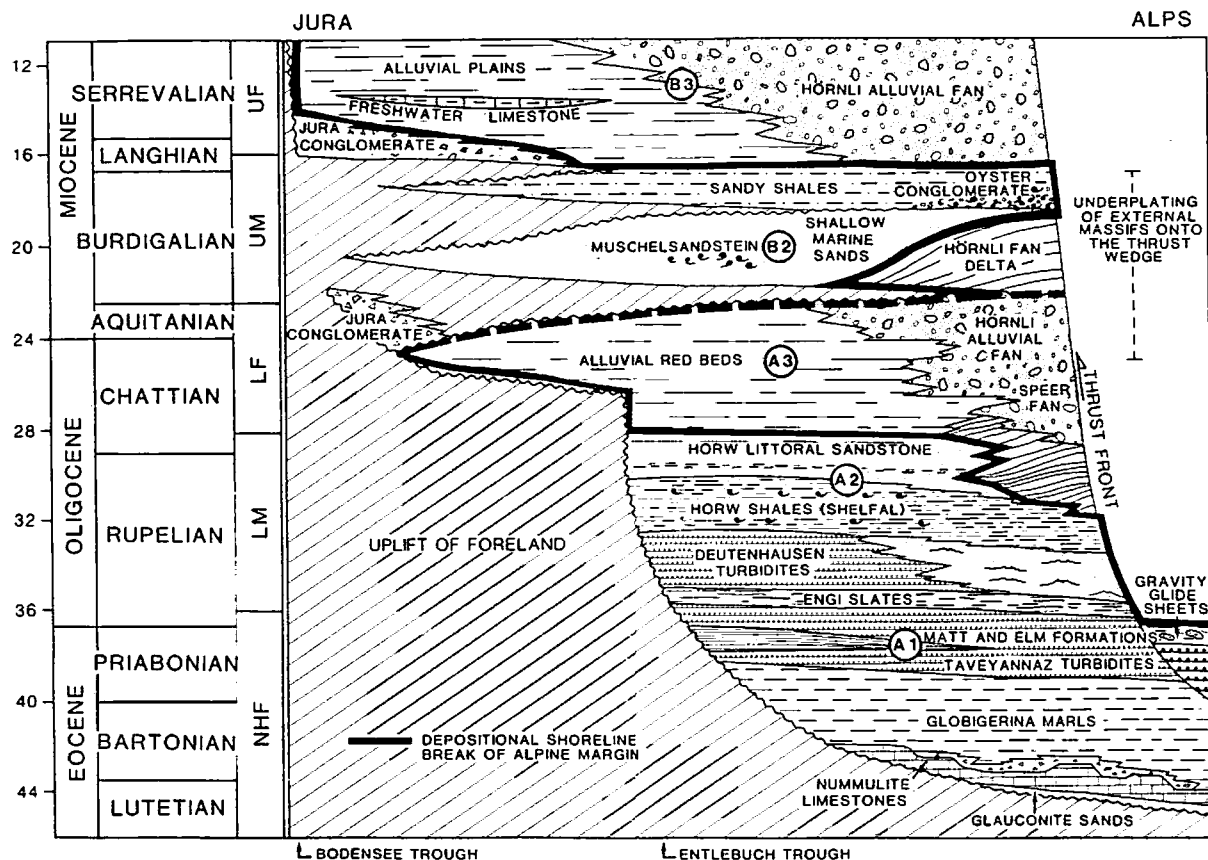


Fig. 2. Chronostratigraphic (Wheeler) diagram of the North Alpine Foreland Basin. The stratigraphy is divided into two shallowing and coarsening upward cycles (A and B) separated by the base Burdigalian (approximately 22 Ma) unconformity. The approximate timing of the underplating of the External Massifs correlates to the cycle boundary.

of these components through time. Ignoring in-plane forces and applied torques (bending moments), the load is the distributed vertical forces imposed by the orogenic wedge plus the basin infill. The plate deflection and the surface slope of the wedge control the redistribution of the load by erosion of material from the mountain belt and sedimentation in the basin. We approximate the process of erosion and deposition by a diffusional law whereby the transport rate is proportional to the topographic gradient [Begin et al., 1981; Kenyon and Turcotte, 1985; Moretti and Turcotte, 1985; Flemings and Jordan, 1989].

Each model is completely described by four parameters (Figure 3): (1) the effective elastic thickness of the foreland plate, (2) the rate of thrust front advance, (3) the surface slope angle of the thrust wedge, (4) the diffusion coefficient. The aims of the model are to investigate the relationship between a developing thrust wedge and the stratigraphic architecture of the associated foreland basin via the diffusion process. In order to keep the system as simple as possible a number of assumptions are necessary with respect to the tectonic and sedimentary processes involved: (1) we assume the lithosphere behaves as an elastic plate overlying an

inviscid fluid, (2) erosion and deposition can be described as a diffusion process, (3) the orogenic load obeys thrust wedge criteria, maintaining a critical taper [Chapple, 1978; Davis et al., 1983], (4) absolute sea level remains constant. On the basis of these parameters and assumptions we model the discontinuous foreland basin stratigraphy, reproducing the primary unconformity separating the two large-scale cycles of the NAFB (Figures 2 and 5a), by invoking close-to-continuous tectonic processes.

THE ALPINE THRUST WEDGE

In our discussion of mountain belt evolution we assume a thrust wedge in dynamic equilibrium [Chapple, 1978; Davis et al., 1983]. The basic mechanical concept is of a noncohesive Coulomb wedge whose taper angle is dictated by the balance between the compressive and gravitational forces against the basal resistance to sliding, which is a function of friction and slope of the underlying decollement surface. The foreland propagation of the wedge is achieved by frontal accretion, which, to maintain the critical taper angle, must be compensated for by

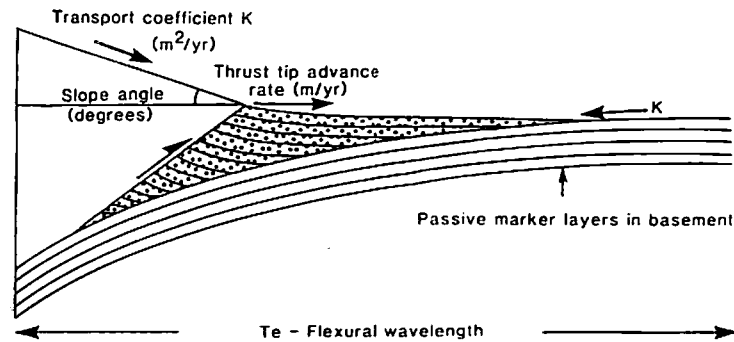


Fig. 3. Representation of the four parameters used in the modeling to simulate the thrust wedge - foreland basin system: (1) flexural rigidity (expressed as equivalent elastic thickness T_e), (2) diffusion coefficient K , (3) thrust wedge advance rate, and (4) topographic slope of thrust wedge.

thickening within the wedge; this is accomplished on faults by backthrusting, out-of-sequence thrusting and underplating of material onto the base of the wedge, or by bulk deformation of the wedge. The internal thickening will be counteracted by erosion of the upper surface.

The evolution of the thrust wedge has been constrained using published data from Pfiffner [1986], who constructed a series of sequentially restored cross sections through the external Alps of eastern Switzerland from the middle Eocene to the present day (Figure 4). These sections utilize all available information on the maximum depths of burial at the base of the wedge, obtained from illite crystallinity on Liassic shales [Frey, 1978]. Pfiffner also used pebble and heavy mineral analyses [Leupold et al., 1942; Tanner, 1944; Mange-Rajetzky, 1985; Allen et al., 1985] to partly constrain the unroofing history of the wedge. Additional geophysical data [Hsu, 1969; Pfiffner et al., 1988] have enabled estimates of the depths to detachment for the external massifs to be made. Figure 4 illustrates the development of the Alpine thrust wedge between 40 and 17 Ma, simplified from Pfiffner [1986]. This demonstrates an initial phase of rapid propagation of the thrust front between 40 and 30 Ma, advancing northward onto the European margin at an approximate rate of 2-4 mm/yr associated with a low angle of taper. The later evolution is characterized by a decrease in thrust front propagation rate and a transfer of the mass influx into the wedge from frontal accretion to internal thickening, dominated by the underplating of the external massifs. The evidence for the timing of underplating comes from isotope work by Hunziker et al., [1986]; the allochthonous cover to the Aar massif was incorporated at this stage into the Helvetic nappes, the deformation being dated as between 30 and 35 Ma using K/Ar and Rb/Sr methods, whereas the underlying autochthon to the massif yields K/Ar dates between 25 and 15 Ma for deformation. This reflects the accretion of the uppermost part of the foreland plate onto the base of the growing thrust wedge approximately 10 m.y. after the initial overthrusting of the area and also correlates with a period of rapid uplift within the wedge between 22 and 18 Ma (work of D. Werner in Rybach [1979, Figure 4]). This period of thickening and rapid uplift in the wedge is also seen in the heavy mineral studies of the basin infill, where the appearance of blue

amphiboles in the late Chattian and Burdigalian marks the exposure of blueschists [Mange-Rajetzky, 1985; Allen et al., 1985].

THE EUROPEAN PLATE

Geological History

In considering the influence of the foreland plate on the basin stratigraphy, the primary factor is the mechanical strength of the lithosphere, which controls the length scale of compensation of an applied load. The strength of the plate is described by the flexural rigidity, or the equivalent elastic thickness. The possible range of values and relevance of the flexural rigidity will be discussed more fully in the section on modeling. For the moment, we need only consider the flexural rigidity as a function of the thermal state and mechanical continuity of the plate.

Heating of the lithosphere is commonly associated with either stretching resulting in a steepening of the geothermal gradient [Burke and Dewey, 1973] or burial during underthrusting in collisional belts [Kominz and Bond, 1986]. The European plate has a complex history of extensional and compressional tectonics. The Hercynian orogeny during the Permian-Carboniferous involved crustal thickening and the intrusion of granitoids with late-stage uplift and erosion. Associated with these late Hercynian events was the formation of a system of SW-NE striking grabens [Bachmann et al., 1987]. The Entlebuch and Bodensee troughs of central and eastern Switzerland are part of this system. The Triassic was a period of relative quiescence when evaporites were deposited which acted as an important decollement horizon during later Alpine compression. The Early to Middle Jurassic marked a period of rifting during which thick carbonate sequences were deposited. By this time, oceanic crust had started forming to the south as part of the Tethyan Ocean. From the Middle Jurassic until the Albian, faulting decreased and limestones and shales blanketed the region. The trend of Jurassic faulting ran parallel to the present strike of the mountain belt in Switzerland. The Tertiary began with regional uplift of the European margin associated with the closure of Tethys

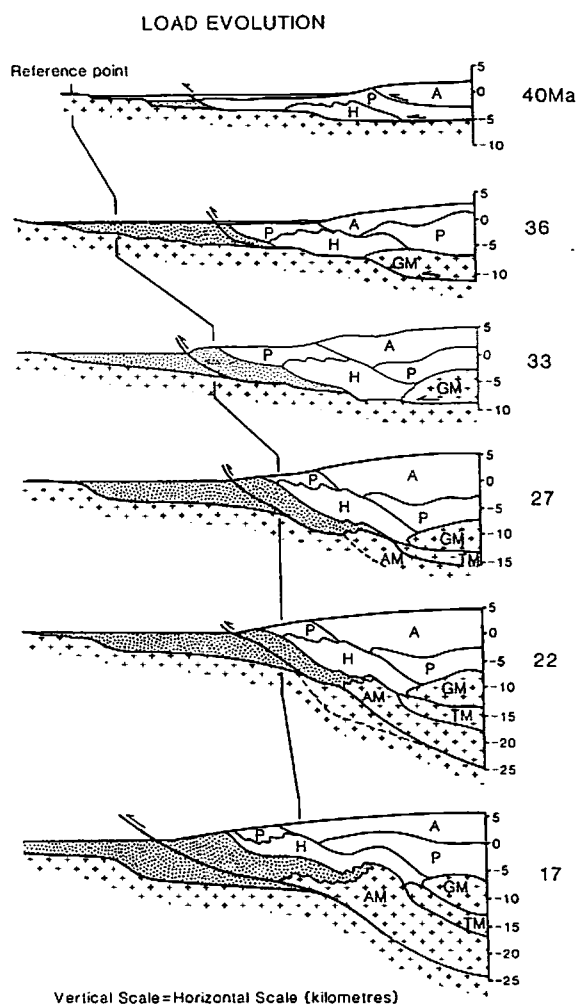


Fig. 4. Sequential restoration of the Alpine thrust wedge of eastern Switzerland, based on Pfiffner [1986]. The reference point in the European plate demonstrates an initial period of rapid wedge advance (2-4 mm/yr) over the plate, followed by thickening of the wedge by underplating of the External Massifs associated with a slowing of the thrust advance rate. Abbreviations are H, Helvetic nappes; P, Penninic nappes; A, Austroalpine nappes; GM, Gotthard Massif; TM, Tavetsch Massif; and AM, Aar Massif.

and the approach of the orogenic wedge from the south. This period is marked by the basal Tertiary unconformity, which Trümpy [1973] termed the "Palaeocene Restoration".

In summary, we are able to distinguish two features of the foreland plate that are considered to influence the development of the North Alpine Foreland Basin: primarily, the relative youth of the basement, and, secondarily, the presence of fundamental fractures in the upper crust, such as the Permian-Carboniferous grabens and Jurassic normal faults. Both of these features predict that the European plate should be relatively weak.

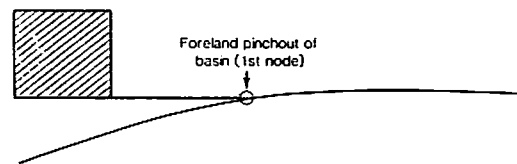
Method for Estimating the Elastic Thickness of the European Plate

Gravity anomalies in mountain belts have been applied to the evaluation of the flexural rigidity of the foreland plate. Karner and Watts [1983] estimated the equivalent elastic thickness (see equation (7)) of the European foreland to be between 25 and 50 km. Lyon-Caen and Molnar [1989] included a terrain correction into the reduction of the gravity data and suggested that the gravity profiles of the Alpine belt, north of the Ivrea body, could be used to constrain the lithospheric strength of the European plate during development of the NAFB. This suggests that the dynamic processes which originally formed the NAFB have now ceased, precluding the use of gravity anomalies in evaluating the flexural rigidity of the European plate [Lyon-Caen and Molnar, 1989].

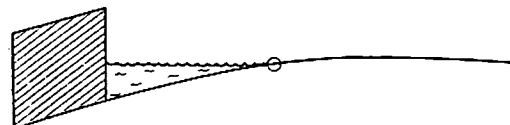
It was necessary to use the stratigraphy of the NAFB to calculate the curvature of the foreland plate and thereby to estimate the strength of the lithosphere during formation of the foreland basin. We used a simple model of end loading on a broken linear elastic plate. By using the reconstructed configuration of the mountain belt at a suitable point in time we combined stratigraphic and structural data to give details of the basin geometry and load configuration, respectively. The methodology of this simple model is illustrated in Figure 5. The load estimated from structural restorations [Pfiffner 1986] at 17 Ma was placed onto the end of the plate, causing an initial deflection and associated peripheral forebulge. The deflection caused by this downwarping was filled with water. The deflection was then filled to sea level with sediment, broadening the distributed load and so pushing the basin and forebulge towards the foreland.

METHODOLOGY FOR SIMPLE MODEL

- ① PLACE ESTIMATED LOAD ON END OF PLATE



- ② DROP LOAD INTO DEFLECTION AND FILL BASIN WITH WATER



- ③ COMPLETELY FILL BASIN WITH SEDIMENT

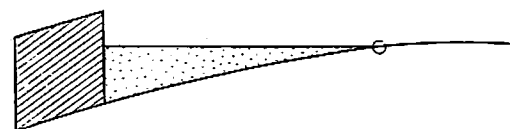


Fig. 5. Methodology for simple model of end loading a plate to evaluate equivalent elastic thickness.

The curvature of the European plate at 17 Ma was ascertained by using 11 decompact sediment columns taken from the restored cross section running north from the Künsnacht borehole, located approximately 10 km south of Zürich [Naef et al., 1985] (Figure 7a). To decompact the depth to basement, we assumed a sandstone lithology throughout and an exponential decrease in porosity with depth. The data points further to the south were estimated from the restored sections of Pfiffner [1986] and have been given broad error bars. The tight curvature of the plate suggests a very weak lithosphere with an equivalent elastic thickness of approximately 10 ± 5 km (Figure 6). The maximum depth to basement of the basin at this time was about 6 km below the thrust front. Varying the magnitude of the load alters the deflection of the plate, without significantly changing the width of the basin. A deflection of 6 km at the thrust front was achieved in the model by assuming the frontal reconstruction of the load to be correct and increasing its mass by placing the free end of the plate further beneath the mountain belt and so extending the hinterland termination of the load. The observed deflection of the plate from the borehole data was matched by using a load width of about 100 km. It was noticeable that any further increase in the overthrust length of the load made negligible difference to the deflection since the underlying plate became near vertical under the mountain belt at large load magnitudes. The value of 10 ± 5 km for T_e at 17 Ma can then be used as a fixed parameter in the diffusion modeling of the NAFB. The rationale behind keeping this value as a constant during the running of the model is based on the long time period (60 m.y. or more) since rifting, allowing almost complete thermal reequilibration, and the lack of any evidence to the contrary.

THE NORTH ALPINE FORELAND BASIN

Present Structural Setting

The present-day structure of the NAFB in eastern Switzerland can initially be divided into two zones: a more

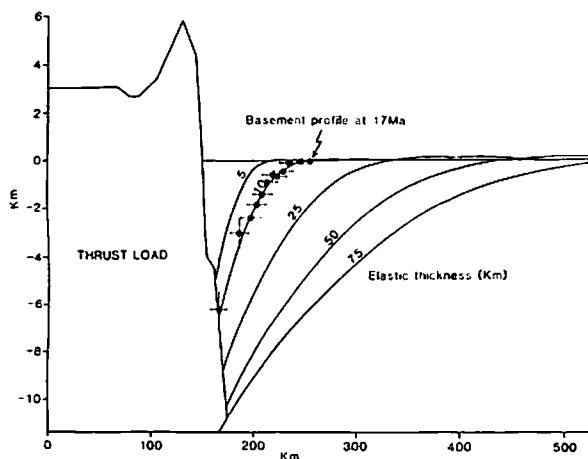


Fig. 6. Estimation of the equivalent elastic thickness (T_e) of the European foreland plate based on the basement configuration at 17 Ma. The observed curvature approximates to a T_e of 10 ± 5 km.

internal, topographically elevated and strongly deformed region to the south and an external, relatively undeformed region to the north, termed the Plateau Molasse (Figure 7). The former contains the sediments of most southerly paleogeographic origin; these are the turbidites of the North Helvetic Flysch (A1), found wrapped around the uppermost Helvetic nappes [Pfiffner, 1981] and in the underlying parautochthonous cover to the Aar massif. The parautochthonous examples are exposed in tectonic windows to the south of the Helvetic nappes (Figure 7b) as seen in the Panixerpass region, Canton Glarus. Between the external Plateau Molasse and the highly deformed region to the south the thickest deposits of the NAFB are steeply tilted within imbricate thrust blocks of the Sub-Alpine zone. North of the Plateau Molasse the sediments thin and pinch out into the Tafeljura.

Stratigraphy

The stratigraphy of the NAFB (Figure 2) exhibits a classical foreland basin succession (*sensu* Covey [1986]), starting at about 42 Ma with an underfilled turbidite dominated "flysch" stage. By 32 Ma the basin was occupied by shallow marine and fluvial deposits. This commences the "Molasse" stage, and similar terrestrial and shallow marine sediments continued to be deposited until approximately 11 Ma when regional uplift of the basin took place.

Four lithostratigraphic groups are traditionally distinguished within the NAFB stratigraphy [Matter et al., 1980]. The basin fill should, however, be extended to include the North Helvetic Flysch to make five groups. These are listed in ascending stratigraphic order: (1) North Helvetic Flysch (NHF), A1; (2) Lower Marine Molasse (UMM), A2; (3) Lower Freshwater Molasse (USM), A3; (4) Upper Marine Molasse (OMM), B2; (5) Upper Freshwater Molasse (OSM), B3.

The parenthetic abbreviations represent the Swiss/German names for the groups as used in previous European literature. For the purposes of this paper we have divided the entire basin into two large-scale shallowing upward cycles, A and B. These two cycles are then subdivided into three paleoenvironmental subunits, representing a simple three-stage breakdown of a regressive succession: 1, deep marine; 2, shallow marine; 3, continental. Using this straightforward scheme, cycle A contains all three stages from deep marine to continental. The base of the Upper Marine Molasse (B2) marks the lower boundary of cycle B and represents a return to shallow marine conditions. This is followed by continental sedimentation during the Upper Freshwater Molasse (B3).

The Palaeocene Restoration: A Forebulge Unconformity?

The first sign of the arrival of the thrust wedge onto the southern margin of Europe is seen at the present day as a break in sedimentation with a maximum chronostratigraphic gap of Middle Jurassic to middle Eocene [Herb, 1988; Allen et al., 1990]. This was described by Trümpy [1973] as the "Palaeocene Restoration". This unconformity underlies the whole basin, separating eroded Tethyan platform carbonates from progressively younger Tertiary sediments as it is traced northwards into the foreland (Figure 2). Herb [1988] has constructed a series of palinspastic restorations of the unconformity, clearly illustrating that as it is traced from Panixerpass through the overlying Helvetic nappes, (i.e.,

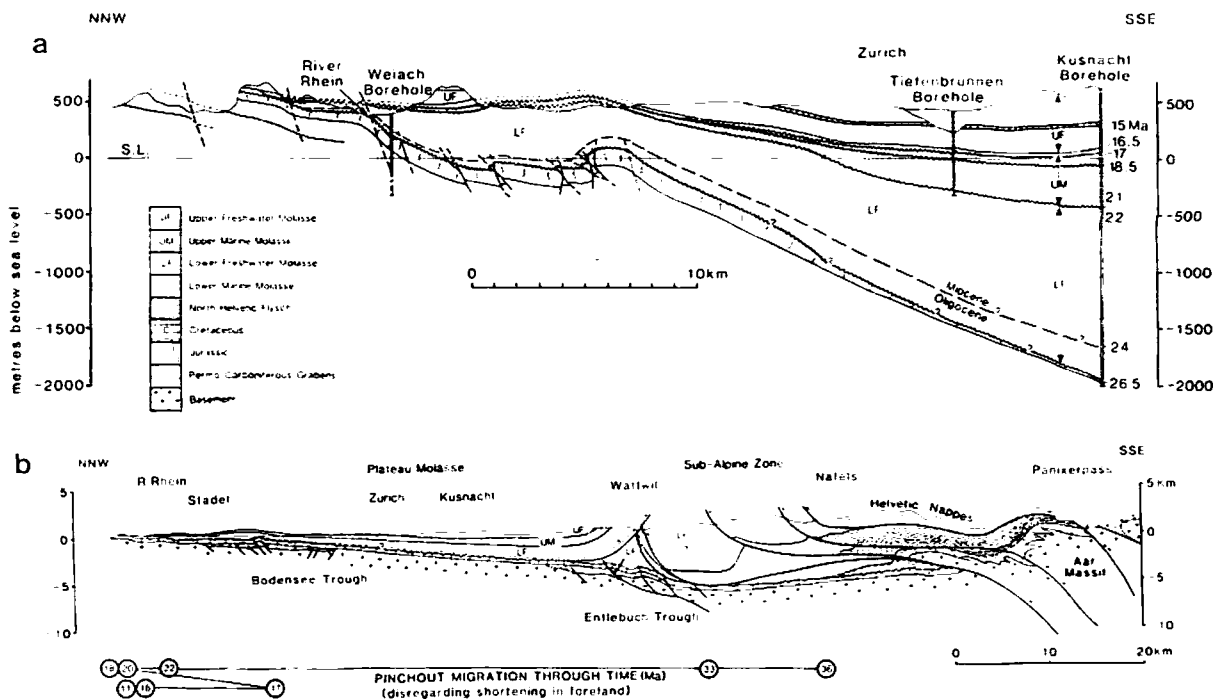


Fig. 7. Structural and stratigraphic sections through the North Alpine Foreland Basin (NAFB) of eastern Switzerland. (a) Detail of outer margin of NAFB from Naef et al. [1985], showing position of unconformities. (b) General cross section showing main structural features of NAFB. Note the locations of the Permian-Carboniferous grabens in the basement [from Vollmayr and Wendt, 1987] relative to the pinchouts in stratigraphy.

heading south in terms of original paleogeography), one observes a decrease in the amount of missing stratigraphy from the Cretaceous and Paleogene [Trümpy, 1980]. Examination of the succession within the Sardona nappe, which is considered to be of more southerly (Ultrahelvetic) origin than the Helvetic nappes [Ruefli, 1959], shows a complete succession through the Cretaceous-Tertiary boundary [Wegmann, 1961].

The North Helvetic Flysch: A1 (42-36 Ma). Deposition occurred during the early Lutetian of 10-50 m of shallow marine nummulitic limestones overlying the basal unconformity (Figure 2) [Styger, 1961]. These grade up into approximately 350 m of Globigerina marls representing water depths of several hundred meters [Herb, 1988]. Above these marls are approximately 2 km of turbidites [Siegenthaler, 1974], the first southerly derived sediments. In both eastern and western Switzerland the oldest of these turbidites (Taveyannaz Sandstones) display evidence of deposition in thrust top (piggyback) basins [Ori and Friend, 1984; Lateltin, 1988; Sinclair, 1989]. The southern margin of the Tavayannaz basin is overlain by a 50-100 m thick olistostrome deposit, indicating its proximity to the thrust wedge.

Lower Marine Molasse: A2 (36-27 Ma). Marine conditions continued into the middle Oligocene, as a narrow branch off Tethys. The stratigraphy and sedimentology of A2 has recently been described by Diem [1986]. It contains thick sequences of marine siliciclastic

deposits now exposed within the imbricate thrust slices of the Sub-Alpine zone. Lower A2 is represented by the Deutenhausen beds of early Rupelian age (P18-P19 foraminifera zones). The Deutenhausen beds comprise about 1 km of delta front channel turbidites and progradational lobe deposits shedding material northwards [Diem, 1986]. Ideally, this lower portion of A2 should be included into A1 due to its deep-water environment, but this would cause confusion with reference to previous literature.

Middle A2 consists of the Horw Shales which comprise 700 m of dominantly shallow marine mudstones rich in ostracods and foraminifera yielding middle Rupelian ages (P20 foraminifera zone). Towards the top of A2 these fine-grained shelf deposits are overlain by a regressive series of coastal sandstones and fan delta conglomerates called the Horw Sandstones, dated at late Rupelian/Chatian (NP24 nannoplankton zone). Work by Diem [1985] on wave ripples from the Horw Sandstones indicates increasing paleowave period and power towards the east, suggesting a funnel shaped basin during A2 deposition. Paleogeographic reconstructions by Büchi and Schlanke [1977] indicate a basin width of 40-50 km during A2, which is in agreement with Diem's data on the wave fetch. Consequently, during A2 we see the filling of a narrow basin from deeper water turbidites to shallow marine and coastal sediments (Figure 2), with the northern margin of the basin containing a thin continental deposit.

Lower Freshwater Molasse: A3 (29-22Ma). At the onset of the Chattian, sedimentation was dominated by seven large alluvial fans coming off the thrust front to the south [Büchi and Schlanke, 1977]. In eastern Switzerland the Rigi and Speer fans shed vast thicknesses (up to 4 km) of conglomerates which are intercalated with silty marls at the lateral limits of the fans. The conglomerates contain material derived from the erosion of Cretaceous Penninic and Ultra-Penninic flysch.

Towards the end of the Chattian, large amounts of epidote entered the system; this arrival of epidote marks the erosion of material involved in the Lepontine greenschist metamorphic event at about 38 Ma, interpreted to reflect rapid uplift within the thrust wedge [Trümpy, 1980]. During the Aquitanian there was a gradual northward shift of the alluvial sediment supply and the development of the Hörnli fan. The Hörnli fan is characterized by abundant dolomitic debris as well as clasts of south and north Helvetic origin such as nummulitic limestones and greensands from the erosion of A1.

A3 is the culmination of cycle A. The underfilled basin containing turbidites and shales was succeeded by coastal and shallow marine sedimentation, finally overflowing to give large thicknesses of fluvial deposits. During this period there was a progressive northward stratigraphic onlap onto the foreland. Although the onlap pattern reveals an initial steady movement of the stratigraphic pinchout during A1 and A2, it is more erratic during A3 (Figure 7). Pfiffner [1986] interpreted much of the rapid thickness changes in A3 as due to active normal faulting during deposition.

Upper Marine Molasse: B2 (22-16 Ma). At the beginning of the Burdigalian, shallow seas flooded the Molasse basin. The southern margin of deposition was located within what is now the Sub-Alpine zone, the northern pinchout remaining in a similar position to that of A3, at present located near the River Rhein. At this time the width of the basin of deposition was approximately 60-80 km. The overall thickness of B2 in eastern Switzerland varies between 200 and 800 m. In the Küssnacht borehole, B2 is approximately 450 m thick.

In Switzerland, sedimentation was dominated by two large deltaic fans, located in positions controlled by earlier fans; in central Switzerland this was the Napf fan, and in eastern Switzerland the Hörnli fan. These deltaic fans were fed by large fluvial systems coming off the thrust wedge and passing northwestward into wave- and tide-dominated marine conditions [Homewood and Allen, 1981]. Petrological studies [Allen et al., 1985] revealed distinct heavy mineral provinces in the Burdigalian seaway and demonstrated that the drainage basin of the Napf fan extended far into the crystalline massifs of the internal Alps, eroding high-pressure minerals from Penninic basement and ophiolites.

The basal unconformity to the B2 transgression indicates initial flooding from the Rhône sea to the west and Paratethys to the east. Berger [1985] dated the basal unconformity using a number of biostratigraphic indicators, including foraminifera and small mammal skeletal debris. He was able to show that the initial bidirectional flooding occurred during the late Aquitanian (NM2b micromammal zone) and that a marine link between the east and west occurred at the Aquitanian/Burdigalian boundary. The deposits of this narrow seaway then started onlapping northwards over the deposits of A3 during the early Burdigalian (NM3).

In the cross section of this study, B2 is divided into three chronostratigraphic subunits dated from the Küssnacht, Tiefenbrunnen, and Weiach boreholes (Figure 7a). Naef et al., [1985] produced a series of subsidence curves and recognized two internal unconformities separating the three subunits of B2. From 22 to 18 Ma, approximately 300 m of shallow marine glauconitic sandstones, limestones, and marls were deposited; this subunit is called the Muschelsandstein and is underlain by a transgressive conglomerate overlying the base Burdigalian unconformity. The base of the Muschelsandstein represents a basinward shift in onlap, followed by renewed northward onlap over the base Burdigalian unconformity described above. At 18 Ma there was a break in sedimentation followed by the deposition of 100 m of sandy shales with a basal oyster-rich conglomerate in the south of the basin, while freshwater conglomerates were deposited in the more northern region of the Weiach borehole. Once again these beds show a basinward shift in onlap onto the underlying Muschelsandstein. At 17 Ma net erosion occurred north of Tiefenbrunnen (Figure 7a), with simultaneous deposition occurring to the south. This bounding surface marks the transition into upper B2 and is marked by a basal conglomerate thinning out north of Küssnacht, followed by 50 m of sandstones.

Upper Freshwater Molasse: B3 (16-11 Ma). Towards the end of the Burdigalian the shallow seas of B2 were filled (Figure 2), with a return to continental sedimentation. The Napf and Hörnli fans remained the main feeder sources in Switzerland, associated with an overall northward shift of the depocenter [Burgisser, 1980; Trümpy, 1980]. These huge alluvial fans drained northwards into longitudinal river systems. In places, thin coal seams and occasional freshwater limestones were deposited. A laterally extensive limestone band dated at 15 Ma is seen within the section of this study (Figures 2 and 7a).

The maximum thickness of B3 is 1500 m, occurring within the centers of the fans, with thicknesses decreasing rapidly northwards. The northern pinchout of B3 is not clear due to erosion, but a glance at the taper of the stratigraphy suggests that it is only slightly north of the pinchout of B2, onlapping onto the Jura [Rigassi, 1977].

STRATIGRAPHIC MODELING

Previous Work

Previous models of foreland basins have reproduced observed stratigraphy simply by applying loads at instants in time on elastic [Jordan, 1981] or viscoelastic plates [Beaumont, 1981; Quinlan and Beaumont, 1984; Beaumont et al., 1988]. The deflection is immediately enhanced, and a new sedimentary layer occupies and expands the basin, filling to a reference surface. However, thrust loading is not episodic and should be considered as a continuous process [Davis et al., 1983; Platt, 1986; Boyer and Geiser, 1987]. The partitioning of deformation within the thrust wedge is dictated by the mechanical requirements of the critically tapered wedge. Modifications to the geometry of the wedge alter the configuration of the distributed load and so influence the resultant deflection.

The interplay between the rate of thrusting which creates space for sediments and the rate of sedimentation or basin filling which also expands the basin is not

represented in previous stratigraphic models. Jordan [1981] modeled the evolution of the Cretaceous Interior Seaway in terms of separate pulses of flexural subsidence as a response to discrete events of load emplacement. Other work [Beaumont, 1981; Quinlan and Beaumont, 1984; Beaumont et al., 1988] considered viscous decay of an initial elastic response, but loads were still emplaced as a series of large blocks over a number of time steps to simulate the development of the orogenic wedge. Thrust loading displaces the lithosphere, creating a sink, as well as providing a sedimentary source to fill the sink. Deposition and erosion redistribute some of the thrust load into the foreland basin. The flexural strength of the underlying lithosphere dictates how these different processes interact over time, with erosion driving uplift and basin filling, and thrust loading depressing the lithosphere. By imposing simple geometrical constraints on the development of the thrust load and using a transport relationship to describe sedimentation as a function of slope we have developed a simple, physically based model. This allows us to directly link the evolution of the thrust wedge and the adjacent foreland basin and to examine this relationship through variations of the model parameters.

Foreland basin stratigraphy has been used as evidence to support both viscoelastic [Beaumont, 1981; Quinlan and Beaumont, 1984; Tankard, 1986; Beaumont et al., 1988] and elastic plate models [Jordan, 1981; Coakley and Watts, 1991]. Recent studies [Beaumont, 1981; Quinlan and Beaumont, 1984; Beaumont et al., 1988; Coakley and Watts, 1991] have focused on the timing, position, and extent of unconformities over the flexural bulge. These unconformities have been cited as support for viscoelastic relaxation of the lithosphere; erosion occurs as the bulge migrates towards the load, uplifting the distal sediments above the reference level. It is possible to develop similar unconformities on an elastic lithosphere through a redistribution or increase of the load [Flemings and Jordan, 1990; Coakley and Watts, 1991], thus presenting an alternative mechanism. Without conclusive documentation of viscoelasticity we assume a simple elastic lithosphere.

It is apparent that an approach which incorporates known sedimentary and tectonic processes is required. Flemings and Jordan [1989] have expanded on the method of Moretti and Turcotte [1985] to apply diffusion equation modeling of erosion and sedimentation to foreland basins. For these models the diffusion equation describes how the topography of the thrust wedge decays and how the basin fills. This change in sediment and thrust load is then used in the flexure equation to determine how the preexisting basin is distorted by the redistribution of the load. Flemings and Jordan [1989] used a simplified version of a thrust wedge with a critical angle of taper, replenishing the load at every time step to maintain a constant, linear topographic profile in the source region. We adopt a similar approach here, seeking to reproduce the stratigraphy of the NAFB using a model which maintains the thrust wedge at a critical taper, as well as a diffusion model of sediment transport.

The Model

Mass transport. The diffusion equation is commonly used to describe transport, where the rate of transport is proportional to the gradient of potential. Both heat

transport down a thermal gradient and the motion of chemical species down an activity gradient can be described by the diffusion equation. Here we use it to describe the transport of sediment down a topographic gradient [Kirkby, 1971; Carson and Kirkby, 1972; Hirano, 1976; Begin et al., 1981; Hanks and Andrews, 1989].

The relationship is based on two assumptions. First, we assume that the amount of material transported through a vertical plane is proportional to the slope at that point:

$$q(x) = -K \partial h / \partial x \quad (1)$$

K is the transport coefficient, h is the topography, q is the amount of material transported, and x is the spatial variable. Second, we assume that volume is conserved, expressed by

$$-\partial h / \partial t = \partial q / \partial x \quad (2)$$

Substituting (1) into (2), we obtain the diffusion equation

$$-\partial h / \partial t = \partial / \partial x [-K \partial h / \partial x] \quad (3)$$

We take K to be a constant, so $dK/dx = 0$, and the expression simplifies to

$$\partial h / \partial t = K \partial^2 h / \partial x^2 \quad (4)$$

Given a topographic profile, we can use this relationship to specify erosion and deposition and so calculate the change in the thrust and sediment load at every point on the x axis. Where $\partial^2 h / \partial x^2$ (topographic curvature) is negative (highs), erosion occurs. Where curvature is positive (lows), deposition takes place. Using the change in load in the flexure equation (5), we can examine how the depositional basin profile changes over time and develop a more complete understanding of foreland basin development.

Isostasy. The equation for the response of a linear elastic beam to vertical loading, in the absence of horizontal in-plane forces and bending moments, reduces to

$$D \frac{d^4 w}{dx^4} + (\Delta \rho) g w = p(x) \quad (5)$$

where D is the flexural rigidity in newton meters, $\Delta \rho$ is the difference between the mantle and infill densities, g is average gravity, w is the deflection, and p(x) is the load in newtons per square meter. The change in the load is the amount added or removed by erosion and deposition, plus the change in the thrust load for that time step, T(x)

$$p = (\partial h / \partial t + \partial T / \partial t) g \rho_s \quad (6)$$

where ρ_s is the density of the load. To compute the flexure we set the infill density to zero, calculating each increment of deflection as air filled.

Thrust wedge. Mountain belts evolve continuously, advancing and rising in opposition to erosion. The evolution of this geometry is controlled by the strength of the overthrust material which rises until it has enough potential energy to advance over the foreland. For this model we adopt a simple dynamic wedge for the overthrust load, defined by two parameters, the topographic slope and

the rate of advance of the wedge tip. The thrust wedge is maintained at constant slope; eroded material is replenished by material brought through the plane at $x = 0$.

All loads, due to thrusting, erosion, and deposition, are added above the initial basement surface and are accounted for in the modeling. The volume of material deposited at every time step is equal to the volume eroded. Conservation of mass, as assumed in diffusion, requires that the sediment density is equal to the load density. This density is taken to be 2650 kg/m^3 , this being high for the sediment load but low for the thrust load. Solving the flexure equation for this load gives the incremental subsidence and uplift for the interval dt . We assume a plate of linear elastic strength. The flexural rigidity D defines the wavelength of regional compensation and is related to the effective elastic thickness T_e by

$$D = ET_e^3/12(1-\nu^2) \quad (7)$$

where D is in newton meters, E is Young's modulus, and ν is Poisson's ratio, which is dimensionless.

The diffusion and flexure equations are solved numerically. Each is treated independently on the same finite difference grid. The diffusion equation is solved using an inherently stable alternating direction technique from Roache [1982, pp. 95-99]. The solution is obtained by marching down the array, calculating every new value as a weighted sum of the previous spatial value for the current time step and the two previous spatial values from the previous time step. Two passes at diffusion, one forward (zero to n) and one backward (n to zero), provide the change in load for the flexure equation. Regional isostatic adjustment due to flexure distorts the topographic profile, modifying the next step in diffusion.

The model is sensitive to the boundary conditions which modify how transport and compensation are achieved. For diffusion we make $\partial h/\partial x(0) = 0$, indicating no transport through the plane at $x = 0$, equivalent to a drainage divide. At the opposite edge of the grid we set $\partial^2 h/\partial x^2(n) = 0$; there is no change in elevation as sediment leaves the system. The flexure equation is solved by back substitution in a five-band matrix. The solution provides values for uplift and subsidence at each point in the grid. The elevations of the stratigraphic horizons and topography are updated by these amounts. Each model layer is the sum of a series of numerical steps representing the previous evolution of the thrust wedge and basin. The number of steps is defined by the magnitude of K and the length of time represented by the layer, more steps for larger K and longer time. This ensures the accuracy of the solutions obtained.

We assume a broken, linear elastic plate with the free end at $x = 0$. Physically this means that no moments are transmitted from the free end of the slab; $d^2w/dx^2(0) = 0$, and that shear force applied at $x = 0$ is equal to the load applied at $x = 0$, $d^3w/dx^3(0) = p(0)$. At the opposite end of the plate we take $w(n) = 0$ and $\partial w/\partial x = 0$, pinning the beam.

Effects of Varying the Parameters

For each model run we specify four parameters, T_e , K , slope angle, and rate of thrust tip advance (Figure 3). The values define the length scale of flexural compensation, the rate of material flux into the thrust

wedge, the rate at which sediments are delivered to the basin, and how the depositional slope evolves through time. The trade-off between how fast the basin is enlarged and how fast it is filled defines the stratigraphy. No one parameter uniquely controls any one aspect of the final basin, each interferes with the others. This feedback complicates the model.

Figures 8 to 11 show how varying these parameters affects the model stratigraphy. Each parameter is assigned four different values, similar to those used in the final model of the NAFB. The models in these figures differ only by the parameter being considered in the figure, all other values being held constant. A reference model ($K = 400.0 \text{ m}^2/\text{yr}$, rate of thrust tip advance = 0.0025 m/yr , $T_e = 20.0 \text{ km}$, slope angle = 1.5°) is included on each figure at the same scale (shown by an asterisk) to provide a reference for comparison.

Each model run is for 10 m.y., which is divided into 10 layers, each representing 1 m.y. The lines plotted in the stratigraphic diagram are isochronous and similar to depositional interfaces, which are preserved beneath the advancing thrust wedge. The succession overlies a basement of passive marker layers, each of which was originally 100 m thick, allowing an assessment of the extent and magnitude of basement erosion. Erosion of underlying passive margin sediments is commonly observed in foreland basins and is recognized in the Alps [Trümpy, 1973; Herb, 1988], the Appalachians [Jacobi, 1981], and in the Colville trough of Northern Alaska [Coakley and Watts, 1991]. Chronostratigraphic (Wheeler) diagrams which plot the age versus the lateral extent of deposition for each layer in the model provide a measure of the rate of basement onlap and erosion through time.

Figure 8 shows the effect of varying the transport coefficient K , from $100.0 \text{ m}^2/\text{yr}$ to $800.0 \text{ m}^2/\text{yr}$. When K is low, sediment transport is inhibited, and the basin remains underfilled. With a low K a steady state is achieved, sediments pond in the central basin, and the position of onlap tracks at a constant distance in advance of the thrust tip. Increasing K fills the basin and onlap exceeds the rate of thrust tip advance. The basin sediments aggrade as deposition climbs onto the flexural bulge. Since the topographic slope of the thrust wedge is held constant, increasing K also enhances the mass flux of material into the rear of the thrust wedge and so increases the basin volume. A further consequence of increased K is that erosion of the flexed plate over the forebulge will be increased.

Flemings and Jordan [1989] compiled a list of determinations of K from a variety of morphological settings; they distinguished between two environments, first, the erosional environment where creep, rill and sheet erosion, and debris flows are dominant and, second, the settings where base flow fluvial processes dominate. The values range over several orders of magnitude, larger values ($10^4 \text{ m}^2/\text{yr}$) are derived from fluvial transport, smaller values ($10^{-2} \text{ m}^2/\text{yr}$) from the decay of isolated slopes. Given that a number of erosional and sedimentary processes are operating synchronously and at different scales in a foreland basin, the precise meaning of the value of K is not clear. In our model we use K to describe the sediment production and slope evolution of the system, encompassing the effects of a number of processes into a single value.

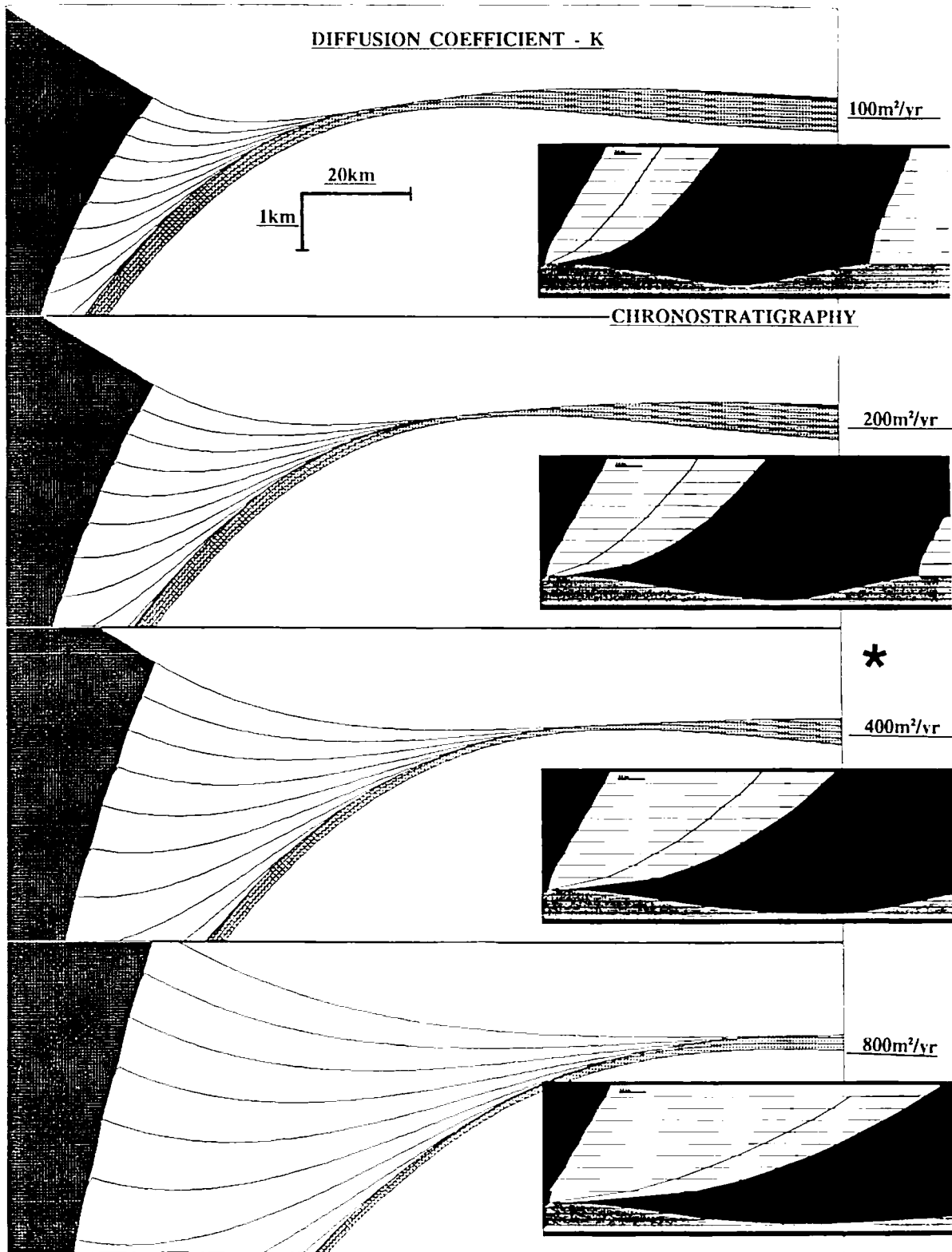


Fig. 8. Influence of varying transport coefficient (K) while holding all other parameters constant. Increasing the value of K causes a broadening and deepening of the deflection while filling it to above regional. "Reference" model shown by asterisk.

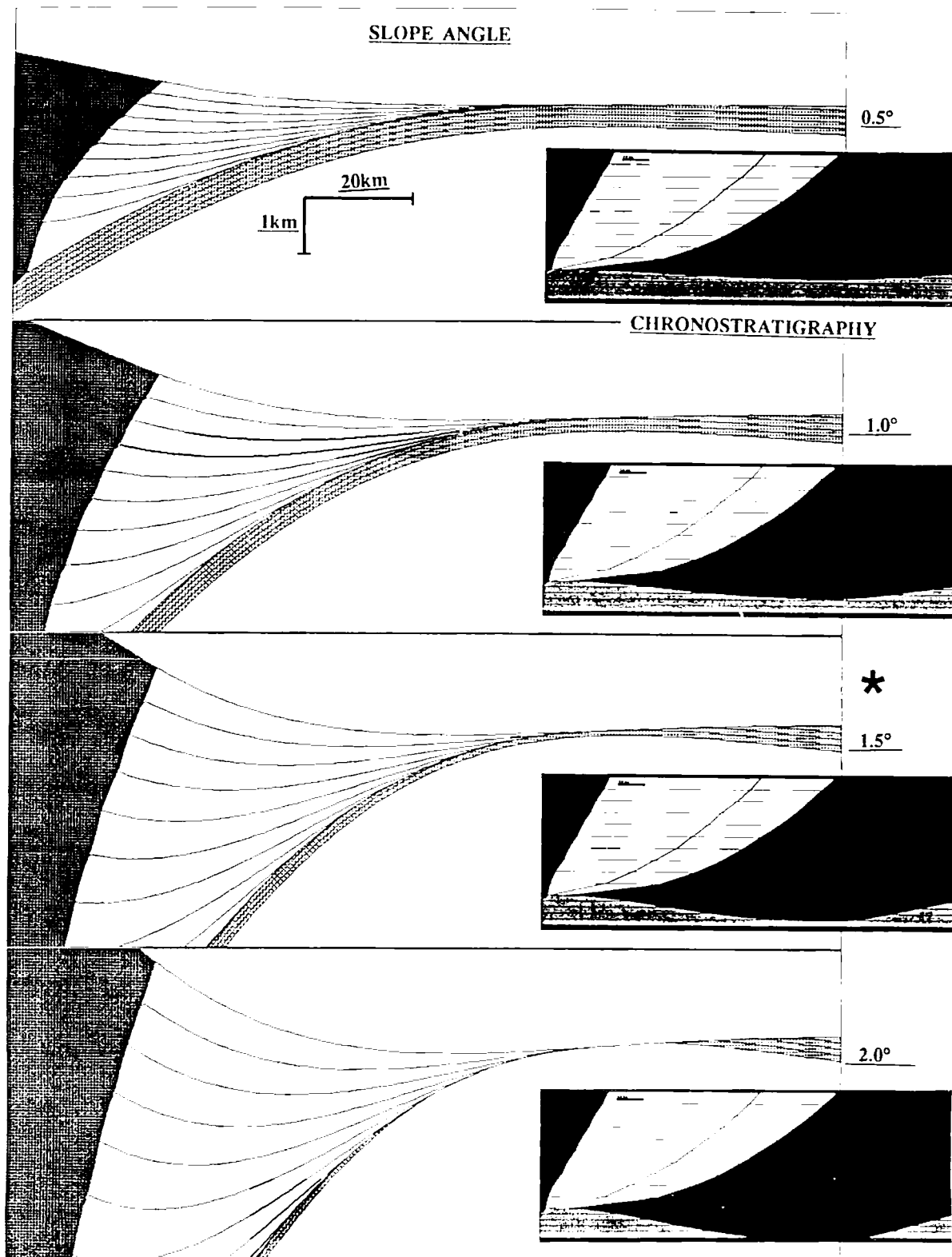


Fig. 9. The influence of varying the surface slope angle of the wedge while keeping all other parameters constant. Increasing slope angle results in a deeper basin but keeps a constant basin width. The increased curvature of the foreland plate associated with the increased slope angle results in increased forebulge erosion. "Reference" model shown by asterisk.

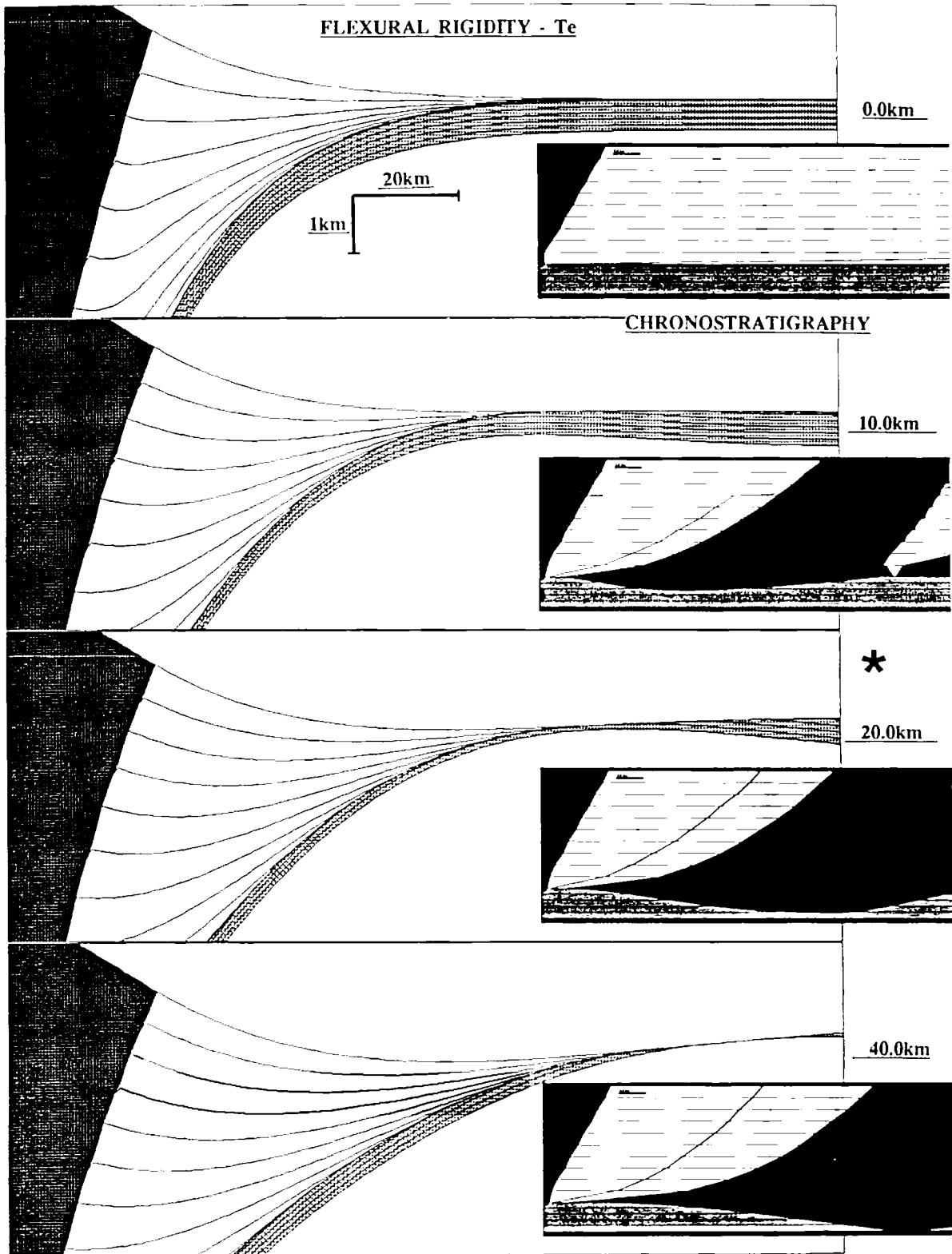


Fig. 10. Influence of varying the effective elastic thickness (T_e) while keeping all other parameters constant. This demonstrates a broadening and shallowing of the deflection with increasing values of T_e . "Reference" model shown by asterisk.

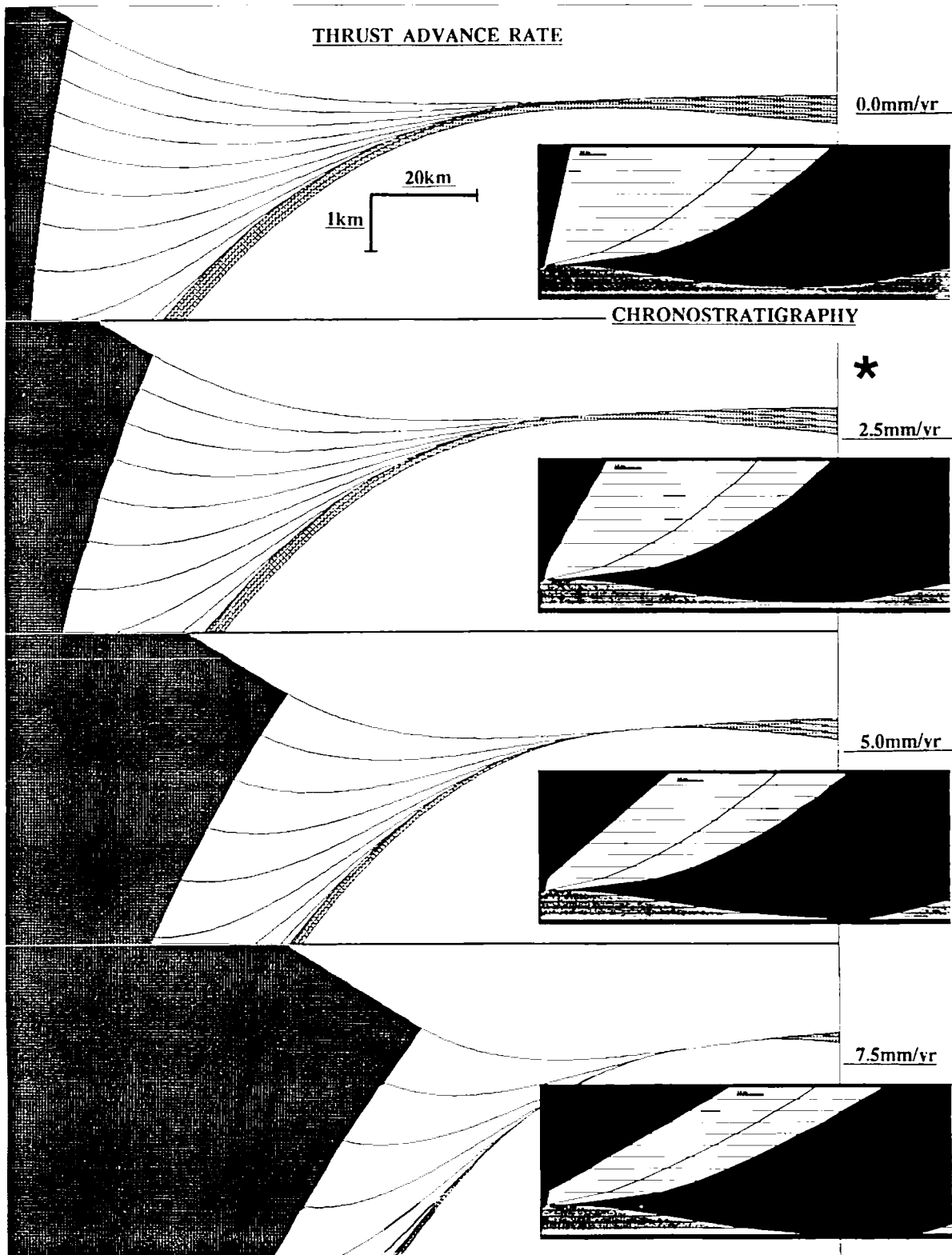


Fig. 11. The influence of varying the thrust advance rate while holding all other parameters constant. Increasing the advance rate results in a narrowing and underfilling of the basin. "Reference" model shown by asterisk.

Figure 9 shows the effect of varying the topographic slope from 0.5° to 2°. The slope defines the rate at which material is brought into the thrust wedge, controlling how deep and how fast the basin develops. Increasing the slope increases the rate at which the load grows and, due to the dependence of the sediment transport on the slope, increases the rate of sediment supply to the basin. The chronostratigraphic diagrams indicate that onlap is approximately the same for each case, illustrating that the sediment and the space in which to put it are generated in constant proportion to each other. The only difference in the chronostratigraphic diagrams is the depth and extent of basement erosion, which is greater for the higher slope. This is due to the larger load which causes steeper slopes in the bulge region, leading to faster erosion of the basement.

Figure 10 shows the effect of varying T_e , which controls the length scale of compensation. T_e is set equal to 0.0 km (Airy case), 10.0 km, 20.0 km, and 40.0 km. These values are low compared to most continents [McNutt et al., 1988] but are similar to those estimated from this paper for the Tertiary evolution of the NAFB. Lower values for T_e cause the trapping of sediment closer to the source, leading to rapid aggradation in a narrow, deep basin. Lower T_e also increases the thickness of the load, since more material is required to maintain a given slope than with a higher T_e . The Airy example exposes a problem in the model. Onlap at each time step marks the dividing line between deposition and erosion. In the Airy case the loading is entirely local and no flexural bulge is created; the depositional slope is a simple decaying exponential from the thrust tip to the right edge of the model.

Figure 11 shows how the rate of thrust tip advance affects the basin geometry. In every thrust belt there is a partitioning of deformation dictated by the energy balance of uplift and advance. This parameter defines the rate at which the entire thrust wedge slides stably over the foreland plate. The rate of thrust tip advance primarily controls the rate at which the load is increased by mass flux through the left hand side of the model. The parameter is varied from 0.0 mm/yr to 7.5 mm/yr in 2.5 mm/yr steps. Rapid advance of the thrust tip creates an underfilled basin. Similar to the case of a low K , onlap tracks at a constant offset from the thrust tip. Lower values allow sedimentation to outpace the creation of space in the basin.

Simulated Model of the North Alpine Foreland Basin (NAFB)

We seek in our modeling to reproduce the broad stratigraphy of the NAFB with the minimum number of parameters and by a minimum variation of those parameters. More complex models are certainly physically justifiable, but lacking independent constraints, we chose a simpler route. Validation of the model is achieved by comparing the volume of the basin infill, the position and timing of the unconformity separating cycles A and B, and the extent and rate of onlap onto the eroded basement.

Lacking a physical rationale for varying T_e and K , both were held constant throughout every model run. The fit was obtained by modifying the transport coefficient and parameters which describe the slope angle and the rate of thrust wedge advance. There are reasons, however, for

believing that T_e and K might vary with time: for example, the Alps overthrust the stretched Tethyan margin [Trümpy, 1980], and stratigraphic models of passive margin development [Steckler and Watts, 1981; Steckler et al., 1988] have been reconstructed in which T_e increases with time since rifting, similar to the oceanic lithosphere [Watts et al., 1980]. The lithosphere cools and strengthens, each sedimentary load achieves compensation on a longer wavelength than that which preceded it, and so stratigraphy oversteps the previous depositional limit, onlapping the passive margin. Stockmal et al. [1986] modeled passive margin overthrusting and found that the resultant foreland basin was insensitive to the age or, equivalently, the strength of the margin immediately beneath it, the compensation of the load being more dependent on the strength of the plate interior. In the case of the Alps, the observed stratigraphy is insufficient to test if the strength of the European lithosphere varied through time, and so T_e was held as a constant.

The parameters that are used to simulate the stratigraphy of the NAFB are based on our understanding of the geological processes involved. The value for T_e is held constant throughout the model at 7.5 km as approximated from the stratigraphy illustrated in Figures 6 and 7a. The value used for the transport coefficient is 500m²/yr, a figure that is intermediate between those thought to typify isolated hillslopes at one extreme and fluvial channel transport at the other [Flemings and Jordan, 1989]. This is considered appropriate as a measure of the long-term transport processes involved on a mountain belt scale comprising both creep, overland flow, debris flow, and base flow (channelized) fluvial transport on a variety of spatial and temporal scales.

The remaining two parameters which characterize the thrust wedge are allowed to vary through time. The rate of thrust front advance has been estimated from Pfiffner [1986] at 2-4 mm/yr during the early development of the NAFB. This value decreases after the main thickening event within the thrust wedge involving the underplating of the External Massifs. The slope of the wedge is constrained by typical topographic slopes for present-day active wedges which range from 1° to 6° [Davis et al., 1983], so defining acceptable limits for the model values.

The model starts at 39 Ma, the time of arrival of the first southerly derived sediments, with a thrust wedge advance rate of 2 mm/yr and with a topographic slope of 2.5°. This parameter pair was run until 24 Ma when the parameters were altered in an attempt to simulate the underplating of the External Massifs. This was done by decreasing the advance rate of the thrust wedge to 0.2 mm/yr and increasing the topographic slope of the wedge from 2.5° to 4° over a period of 200,000 years. After this thickening event the advance rate was increased to 2 mm/yr.

The results of this model are illustrated in Figures 12 to 16. During the interval 39-24 Ma we see the development of the bulk of cycle A. During the initial stages of development the deposits do not fill the basin to a horizontal, indicating that the basin was underfilled. The basin width during this underfilled stage was between 40 and 50 km. As the basin develops, forming the upper part of cycle A, stratigraphic onlap onto the foreland outpaces the rate of thrust advance, resulting in a broadening of the basin to a maximum of 100 km. This rapid onlap over the foreland is a consequence of filling of

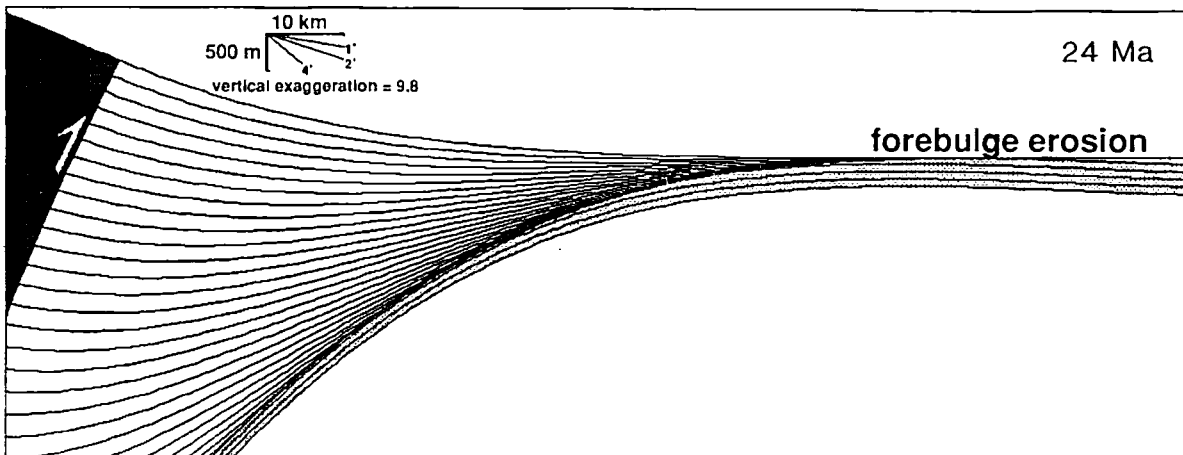


Fig. 12. Simulated stratigraphy of the North Alpine Foreland Basin at 24 Ma. The parameters were held constant from 39 Ma with the value for T_e at 7.5 km, $K = 500\text{m}^2/\text{yr}$, advance rate of 2 mm/yr, and a slope angle of 2.5° . The resultant stratigraphy infills a basin of about 100 km width, which is filled above sea level. At the initial stages of development the basin was relatively underfilled, resulting in significant forebulge erosion as can be seen under the basin. This diagram simulates the overfilled stage of the basin during A3.

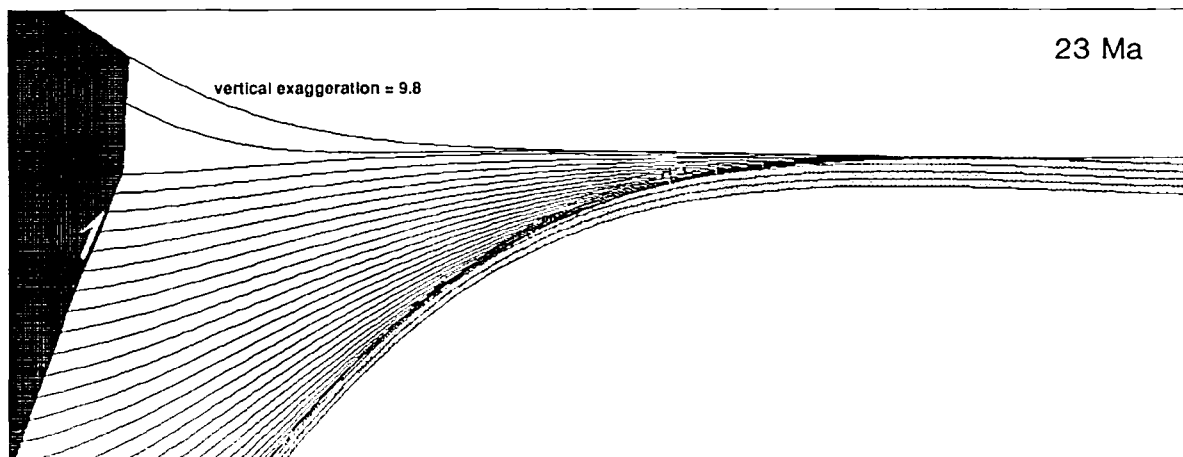


Fig. 13. Simulated stratigraphy of the North Alpine Foreland Basin at 23 Ma. The parameters describing the thrust wedge were altered at 24 Ma to simulate the underplating of the external massifs. The rate of wedge advance was slowed from 2 mm/yr to 0.2 mm/yr, and the surface slope was increased from 2.5° to 4° over a time period of 200,000 years. The sediments deposited during and immediately after this change in the geometry of the thrust wedge are ponded near to the thrust front, with erosion occurring over the forebulge.

the deflection during the evolution from an underfilled "flysch" stage to an overfilled "molasse" stage. The filling of the basin broadens the sediment load which pushes the forebulge out and, at the same time, fills the deflection to above sea level; both processes cause increased progradation of sediments over the foreland.

At 24 Ma the underplating of the External Massifs was simulated by the slowing down and thickening of the thrust wedge. For modeling purposes this thickening is

achieved rapidly, over 200,000 years, whereas we envisage the process as taking place over a longer time span. However, the duration used in the model is that required to reproduce the geological observations. This thickening concentrates the load in the wedge interior, causing backtilting of the basin succession towards the thrust front. Sedimentation is then confined near the thrust front, and diffusion of sediment then starts to progressively fill the basin to its distal limits (Figure 13).

The resultant stratigraphy illustrates a marked unconformity which becomes laterally conformable at about 30 km into the basin (Figures 14 and 15). The stratigraphy of cycle B overlying the unconformity shows a basinward shift in onlap relative to the underlying stratigraphy. This simulates the base Burdigalian unconformity separating cycles A and B, which is clearly illustrated by comparing the observed and calculated onlap on a chronostratigraphic diagram (Figure 15). The thickness of cycle A preserved beneath the unconformity has also been closely matched in the simulation (Figure 16).

The model effectively reproduces both the volume and extent of cycle A, demonstrating its utility, and validating values of the three adjustable parameters that produced it. By reproducing the onlap rate (Figure 15) we demonstrate that both the transport coefficient and the history of thrust advance are compatible with the observed stratigraphy, since onlap rate is only a weak function of the topographic slope (Figure 9). By reproducing the volume of sediments over the interval of cycle A (Figure 16) we demonstrate that both the load size, which defines the deflection, and the amount of sediment generated are compatible with the observed stratigraphy, validating both the wedge slope used and again the transport coefficient. It is important to recognize that the model reproduces the history of cycle A, not merely its geometry.

Figure 14 illustrates the amount of erosion of the modeled foreland plate due to forebulge uplift prior to the progradation of the foreland basin sediments. The maximum erosion (120 m) of the foreland plate occurred during the early underfilled stage. Later erosion of the forebulge was less severe due to rapid progradation of shallow marine and continental sediments. This basal unconformity simulates the geometry of the "Palaeocene Restoration" unconformity underlying the NAFB which shows rapid truncation through the Cretaceous sequence underlying A1 [Herb, 1988; Allen et al., 1990], but steady truncation down to the Jurassic Malm underneath the later overfilled sediments of the basin.

DISCUSSION

There are two aspects of the simulated model which differ significantly from the observed stratigraphy of the NAFB: (1) the thickness of the simulated stratigraphy above the unconformity varies from that of the observed thickness of cycle B and (2) the unconformities within B2 at 18 Ma and 17.5 Ma have not been simulated. These two problems can be addressed by considering, first, the suitability of the diffusion law to describe the erosion, transport and deposition of sediments from mountain belts into their adjacent foreland basins. Second, we must consider the adequacy of surface slope angle as a parameter to describe the kinematics of the critical angle of taper of orogenic wedges.

The diffusion law enables us to use a single parameter to describe the rate of mass transport as a function of local gradient. Variations in the value of the transport coefficient will result dominantly from climatic fluctuations and varying source rock lithologies. Flemings and Jordan [1989, Table 1, p. 3853] suggest that a reasonable range of values for transport coefficients in mountain belts would be from 100 to 5000 m²/yr and for the adjacent foreland basin, from 1000 to 25000

m²/yr. It is also recognized that if we are considering the evolution from a submarine to continental thrust wedge, the values for the transport coefficient will differ significantly. Pinet and Souriau [1988] studied worldwide continental erosion on varying time scales and concluded that the dominant control on long term (10² m.y.) continental denudation is the relief; environmental factors such as climate are important on shorter time scales (< 2 m.y.).

With the large number of possible influences on the value of transport coefficient mentioned above, we must assume that to keep a value of 500 m²/yr as a constant over a period of 20 m.y. in our modeling of the NAFB is simplistic. In realizing the limits of our understanding of values for transport coefficient it is considered imperative that it is held constant, enabling the influence of the evolution of the thrust wedge to be clearly assessed.

The simulated model of the NAFB was stopped at 18 Ma, just prior to the formation of the two unconformities seen within B2. Previous attempts had been made at simulating the upper unconformities within B2 by further increasing the slope angle of the thrust wedge; but these involved excessive increases in the mass influx into the rear of the wedge over short time intervals. Sediment overproduction also became a problem with higher slope angles, hence we did not attempt to simulate the true thickness of the incompletely preserved cycle B. This overproduction may be caused by a number of factors such as: (1) sediment being bypassed out of the NAFB during periods of overfilling, (2) increasing surface slope is not a suitable representation of underplating in thrust wedges (see below), (3) sediment transport is not as directly linked to wedge slope as assumed by this model.

The base Burdigalian unconformity is attributed to changes in the spatial distribution of the load involving addition of material towards the rear of the wedge by underplating. The critical taper of an orogenic wedge is in dynamic equilibrium with three parameters: (1) the mechanical strength of the wedge, (2) the basal friction on the wedge, (3) the density of the wedge [Davis et al., 1983]. If any of these are altered, the critical taper will adapt to compensate. In this paper we have modeled the incorporation of the External Massifs into the Alpine thrust wedge by increasing the surface slope angle of the wedge, representing an increase in critical taper. The increase in surface slope angle causes an increase in sedimentation rates as governed by the diffusion law. But it is important to recognize that the relatively high density of the External Massifs compared to the bulk of the thrust wedge could cause a decrease in topographic slope. The lack of necessity to increase the slope is due to a greater degree of isostatic adjustment in the rear of the wedge, resulting in an increase in the dip of the basal decollement, which, because critical taper is preserved, may reduce the topographic slope correspondingly [Davis et al., 1983]. Therefore we have to recognize that the modeling of the thrust wedge in terms of a single density, with slope angle reflecting alterations in the kinematics of the orogenic wedge, is simplistic.

Figure 17 summarizes some of the qualitative aspects of the geological interpretation of the model. This interpretation satisfactorily accounts for (1) the onlap of Lower Freshwater Molasse (A3) sediments onto the European plate with alluvial fans at the proximal (Alpine) edge of the basin passing downstream into low gradient floodplains and lakes, (2) the erosional hiatus in distal

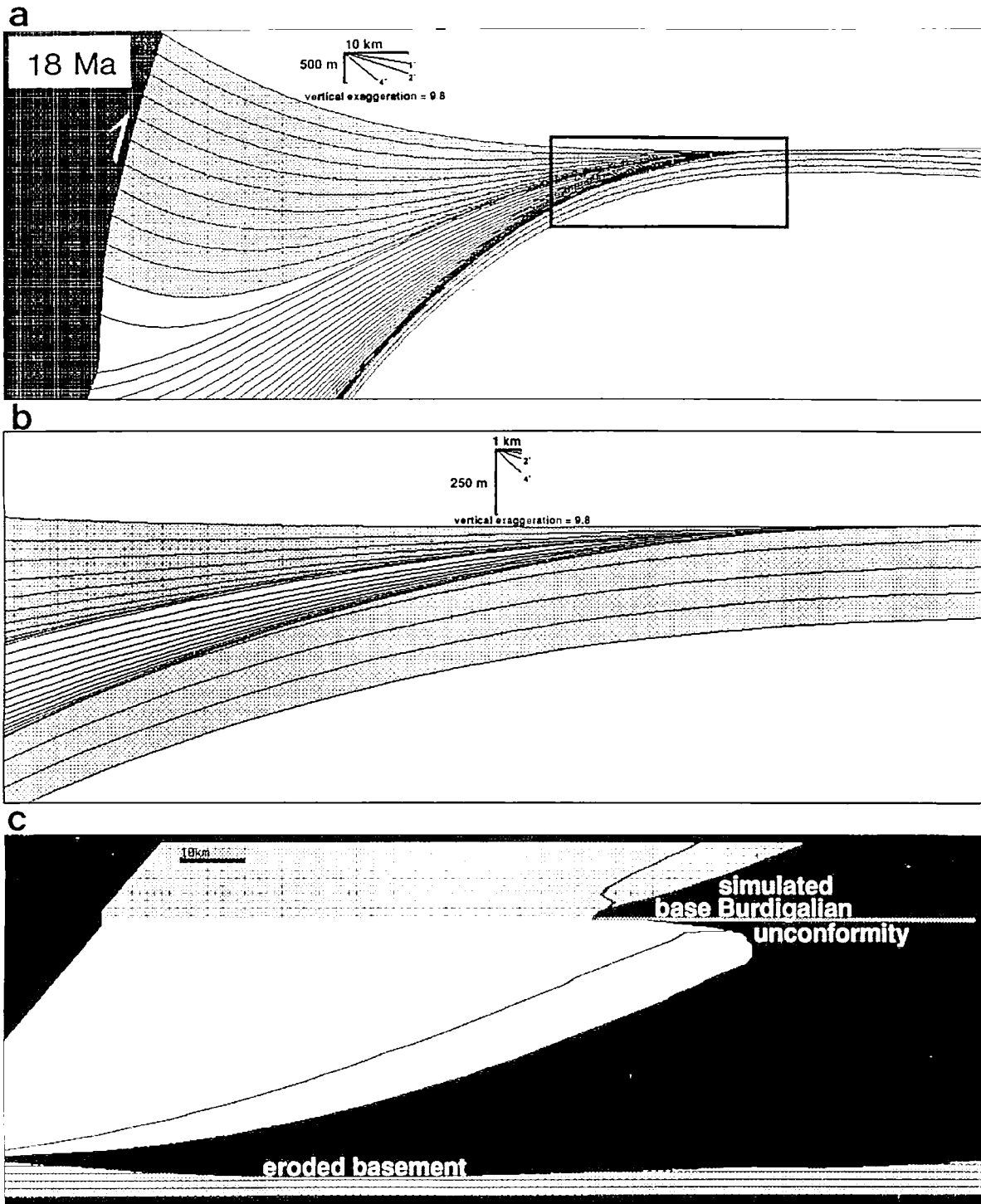


Fig. 14. Simulated stratigraphy of the North Alpine Foreland Basin (NAFB) at 18 Ma. (a) Broad geometry of the basin, with the shaded upper part of the stratigraphy representing the initial sediments of cycle B. (b) Close-up of Figure 14a showing the geometry of the simulated unconformity. The lines in the basement represent 100 m intervals indicating 100-200 m of erosional truncation on the foreland plate due to forebulge uplift. The stratigraphy underlying the unconformity is truncated in the region of the pinch-out and then overlain by the upper succession (shaded) which again onlaps onto the foreland. (c) Chronostratigraphic (Wheeler) diagram of the simulated stratigraphy illustrating the initial onlap towards the foreland of the lower succession, which is then truncated forming an unconformity and resulting in a basinward shift in the position of onlap. This is then followed by renewed onlap of the upper succession. A comparison is made between the simulated and observed onlap of the NAFB in Figure 15.

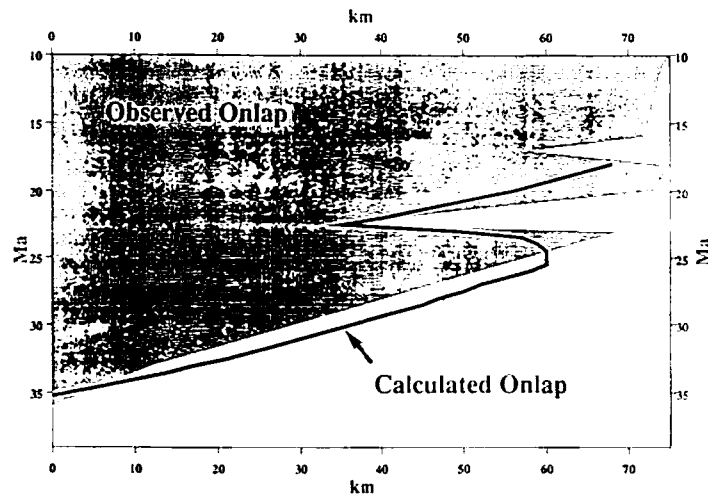


Fig. 15. Comparison of observed onlap from the North Alpine Foreland Basin and that calculated in the simulated model. The basinward shift in onlap at 22 Ma corresponds to the base Burdigalian unconformity.

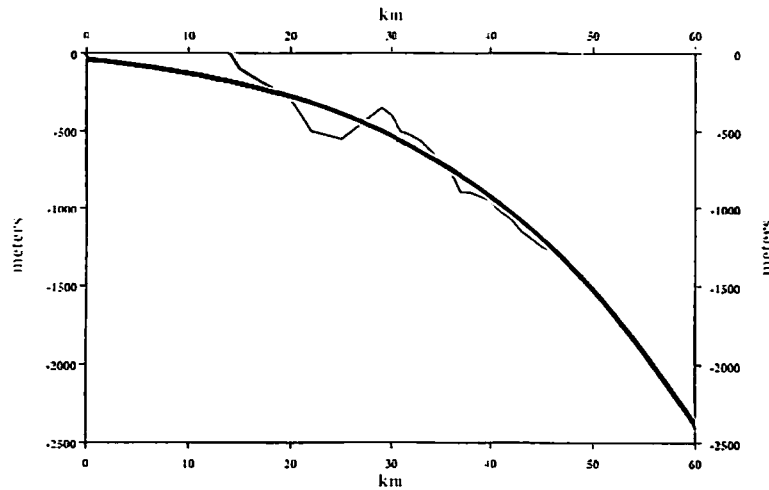


Fig. 16. Comparison of the observed thickness of cycle A preserved below the unconformity (jagged line) and that simulated in the model (thicker line).

positions at the base of the Upper Marine Molasse (B2) passing into a conformity associated with deepening in proximal positions (this deepening provided accommodation space for fan deltas (e.g., Hörnli) to prograde into a marine basin) and (3) the renewed progradation of alluvial fan and fluvial systems towards the north during B3. These qualitative aspects should now be more rigorously tested.

CONCLUSIONS

1. The stratigraphy of the NAFB can be divided into two shallowing and coarsening upward cycles separated by an

unconformity (base Burdigalian, approximately 22 Ma).

2. The Alpine thrust wedge of eastern Switzerland has been sequentially restored [Pfiffner, 1986]. The restoration shows an initial period of rapid thrust wedge advance northward over the European plate from 40 Ma to approximately 24 Ma. At approximately 24 Ma there was a slowing down and thickening of the thrust wedge during underplating of the External Massifs.

3. The equivalent elastic thickness of the continental lithosphere that best fits the observed basement configuration flanking the 17 Ma load approximates 10 ± 5 km. This value is within the range of determinations obtained by Royden [1987] for the Apennines but is significantly less than estimates from the Appalachians

reproduced by a change in the parameters describing the thrust wedge in an attempt to simulate the underplating of the External Massifs. This is achieved by decreasing the thrust advance rate to 0.2 mm/yr and increasing the surface slope angle from 2.5° to 4° over a period of 200,000 years.

7. The renewed stratigraphic overlap of cycle B was simulated by renewing the advance of the thrust wedge from 0.2 to 2 mm/yr and by keeping all the other parameters the same. However, overlap would also occur, though at a different rate, simply by diffusion of sediment from the eroding and recently thickened wedge into the basin without any change in the wedge advance rate. This property makes the linkage between onlap rate and wedge advance rate complex, and the former cannot be used as a proxy for the latter.

8. The base Burdigalian unconformity separating the two large-scale cycles of the NAFB can be simulated by geologically acceptable modifications in the geometry of the thrust load moving over a linear elastic plate. This unconformity is reproduced without recourse to eustasy or anastatic behavior of the continental lithosphere following loading.

ACKNOWLEDGMENTS. H.D.S. carried out this work while on a Natural Environment Research Council funded studentship. Thorough reviews by Peter Fleming and Finn Surlyk are gratefully acknowledged.

REFERENCES

Allen, P.A., M. Mange-Kajczyk, A. Maller and P. Homewood, Dynamic paleogeography of the open Burdigalian seaway, Swiss molasse basin, *Ecologe Geol. Helv.*, 78(2), 351-381, 1985.

Allen, P.A., S. Crampion and H.D. Sinclair, The inception and early evolution of the North Alpine foreland basin, Eastern Switzerland, paper presented at 13th International Sedimentological Congress, Nottingham, England, 26-31 Aug 1990.

Bachmann, G.H., M. Müller and K. Weggen, Evolution of the Molasse Basin (Germany, Switzerland), *Tectonophysics*, 137, 77-92, 1987.

Beaumont, C., The evolution of sedimentary basins on a visco-elastic lithosphere: Theory and examples, *Geophys. J. R. Astron. Soc.*, 55, 471-497, 1978.

Beaumont, C., Foreland basins, *Geophys. J. R. Astron. Soc.*, 65, 291-329, 1981.

Beaumont, C., G. Quinlan, and J. Hamilton, Orogeny and stratigraphy: Numerical models of the Paleozoic in the Eastern Interior of North America, *Tectonics*, 7, 389-416, 1988.

Beggs, Z.B., D.F. Meyer, and S.A. Schumm, Development of longitudinal profiles of alluvial channels in response to base-level lowering, *Earth Surf. Processes Landforms*, 6, 49-68, 1981.

Berger, J.-P., La transgression de la molasse marine Supérieure (OMM) à Suisse Occidentale, *Munchner Geowissenschaftliche Abhandlungen: Reihe A, Geologie und Paläontologie*; vol. 5, Verlag Friedr. Vieweg, München, 1985.

Boyer, S.E. and P.A. Geiser, Sequential development of thrust belts: Implications for mechanics and cross-section balancing, *Geol. Soc. Am. Abstr. Programs*, 597, 1987.

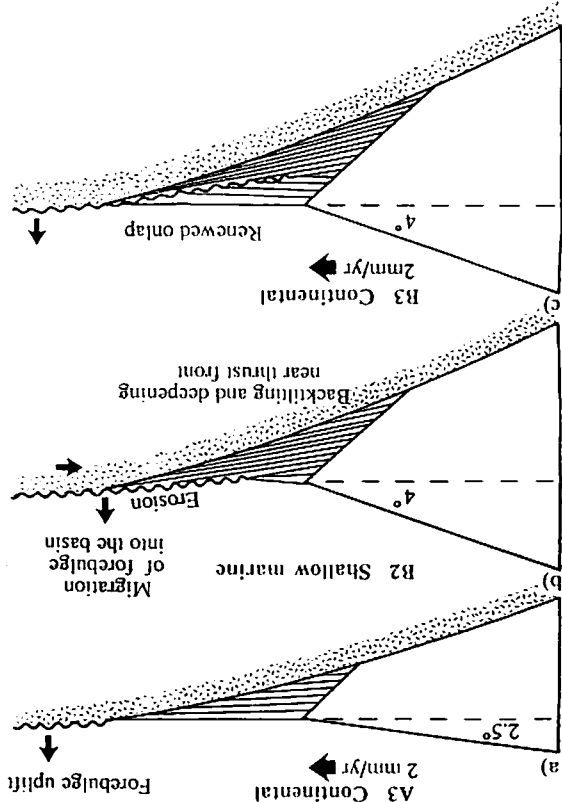


Fig. 17. Schematic diagram to show the mechanism by which the simulated stratigraphy in Figures 12 to 16 was reproduced. (a) Rapid advance of a low angle thrust wedge, and the deposition of the lower cycle. (b) Thickening and slowing down of the thrust wedge causes migration of the forebulge into the basin, with uplift and erosion of the underlying succession. Sedimentation is confined near the thrust front, resulting in a basinward shift in stratigraphic onlap. Backfolding of the basin also causes increased subsidence near the thrust front, resulting in marine sedimentation. (c) Renewed advance of the wedge; keeping the slope angle constant results in filling of the basin, the return to continental deposition, and steady stratigraphic onlap over the foreland.

and Ganges basins [e.g., Jordan, 1981; Karner and Wills, 1983].

4. We consider the development of foreland basins in terms of four parameters: (1) equivalent elastic thickness of the foreland plate (T_e); (2) the rate at which sediment is deposited from the thrust wedge and deposited in the basin, described using a transport coefficient (K) and governed by a diffusion law; (3) the rate of advance of the thrust wedge; (4) the surface slope angle of the thrust wedge.

5. The NAFB stratigraphy was simulated by varying the parameters that describe the evolution of the thrust wedge and by keeping the values of T_e and K constant at 7.5 km and 500 m²/yr respectively. Basin width and stratigraphic thickness for cycle A were simulated using the values of T_e and K described above, with a time-averaged thrust advance rate of 2 mm/yr, and a slope angle of 2.5°.

6. The geometry of the base Burdigalian unconformity is

- Büchi, U.P. and S. Schlanke, Zur paläogeographie der Schweizerischen Molasse, *Erdol Erdgas Z.*, 93 (Spec. Issue), 51-69, 1977.
- Bürgisser, H.M., Zur Mittel-Miozänen Sedimentation im Nordalpinen Molassebecken: das "Appenzellergranit" - Leitniveau des Hörnli Schuttfächers (Obere Süswassermolasse, Nordostschweiz), *Mitt. Geol. Inst. Eidg. Tech. Hochsch. Univ. Zürich, N.F.* 232, 196 pp, 1980.
- Burke, K. and J.F. Dewey, Plume generated triple junctions: Key indicators in applying plate tectonics to old rocks, *J. Geol.*, 81, 406-433, 1973.
- Carson, M.A. and M.J. Kirkby, *Hillslope Form and Processes*, 475 pp., Cambridge University Press, New York, 1972.
- Chapple, W.M., Mechanics of thin-skinned fold and thrust belts, *Geol. Soc. Am. Bull.*, 89, 1189-1198, 1978.
- Coakley, B.J. and A.B. Watts, Tectonic controls on the origin of unconformities, North Slope, Alaska, *Tectonics*, in press, 1991.
- Covey, M., The evolution of foreland basins to steady state: Evidence from the Western Taiwan Foreland Basin, in *Foreland Basins*, edited by P.A. Allen and P. Homewood, *Spec. Publ. Int. Assoc. Sedimentol.*, 8, 77-90, 1986.
- Davis, D., J. Suppe and F.A. Dahlen, Mechanics of fold and thrust belts and accretionary wedges, *J. Geophys. Res.*, 88, 1153-1172, 1983.
- Diem, B., Analytical method for estimating palaeowave climate and water depth from wave ripple marks, *Sedimentology*, 32, 705-720, 1985.
- Diem, B., Die Untere Mesozoische Molasse zwischen der Saane (Westschweiz) und der Ammer (Oberbayern), *Eclogae Geol. Helv.* 79(2), 493-559, 1986.
- Flemings, P.B. and T.E. Jordan, A synthetic stratigraphic model of foreland basin development, *J. Geophys. Res.*, 94, 3851-3866, 1989.
- Flemings, P.B. and T.E. Jordan, Stratigraphic modelling of foreland basins: Interpreting thrust deformation and lithosphere rheology, *Geology*, 18, 430-434, 1990.
- Frey, M., Progressive low grade metamorphism of a black shale formation, Central Swiss Alps, with special reference to pyrophyllite and margarite bearing assemblages, *J. Petrol.*, 19, 93-135, 1978.
- Hanks, T.C. and D.J. Andrews, Effect of far-field slope on morphologic dating of scarp-like landforms, *J. Geophys. Res.*, 94, 565-573, 1989.
- Haq, B.U., J. Hardenbol and P.R. Vail, Chronology of fluctuating sea-levels since the Triassic (250 Myr ago to present), *Science*, 235, 1156-1167, 1987.
- Herb, R., Eocene paläogeographie und paläotektonik des Helvetikums, *Eclogae Geol. Helv.*, 81(3), 611-657, 1988.
- Hirano, M., Mathematical model and the concept of equilibrium in connection with slope, shear ratio, quantitative slope models, *Z. Geomorphol., Suppl.*, 25, 50-71, 1976.
- Homewood, P. and P.A. Allen, Wave-, tide- and current controlled sandbanks of Miocene molasse, western Switzerland, *AAPG Bull.*, 65, 2534-2545, 1981.
- Hsu, K.J., Thin-skinned plate tectonics during Neo-alpine orogenesis, *Am. J. Sci.*, 279, 353-366, 1969.
- Hunziker, J.C., M. Frey, N. Clauer, R.D. Dallmeyer, H. Freidrichsen, P. Roggwiler and H. Schwander, The evolution of illite to muscovite: mineralogical and isotopic data from the Glarus Alps, Switzerland, *Contr. Mineral Petrol.*, 92, 157-180, 1986.
- Jacobi, R.D., Peripheral bulge - A causal mechanism for the Lower/Middle Ordovician unconformity along the western margin of the northern Appalachians, *Earth Plant. Sci. Lett.*, 56, 245-251, 1981.
- Jordan, T.E., Thrust loads and foreland basin evolution, Cretaceous, western United States, *AAPG Bull.*, 65, 2506-2520, 1981.
- Karner, G.D. and A.B. Watts, Gravity anomalies and flexure of the lithosphere at mountain ranges, *J. Geophys. Res.*, 88, 10449-10477, 1983.
- Kenyon, P.M. and D.L. Turcotte, Morphology of a delta prograding by bulk sediment transport, *Geol. Soc. Am. Bull.*, 96, 1457-1465, 1985.
- Kirkby, M.J., Hillslope process - Response models based on the continuity equation, *Spec. Publ. Trans. Inst. B. Geogr. Publ.* 3, 1971.
- Kominz, M.A. and G.C. Bond, Geophysical modelling of the geothermal history of foreland basins, *Nature*, 320, 252-256, 1986.
- Lateltin, O., Les dépôts turbiditiques oligocènes d'avant pays entre Annecy (Haute Savoie) et la Saane (Suisse), Thesis 949, 127 pp., Univ. of Fribourg, pp.127, Fribourg, Switzerland, 1988.
- Leupold, W., H. Tanner and J. Speck, Neue Geröllstudien in der Molasse, *Eclogae Geol. Helv.* 35, 235-246, 1942.
- Lyon-Caen, H. and P. Molnar, Constraints on the deep structure and dynamic processes beneath the Alps and adjacent regions from an analysis of gravity anomalies, *Geophys. J. Int.*, 99, 19-32, 1989.
- Mange-Rajetzky, M.A., Unroofing of orogenic belts as evidenced by heavy minerals in their foreland sediments: An example from the Peri-alpine molasse, paper presented at International Symposium on Foreland Basins, (IAS-SEPM), Fribourg, Switzerland, Sept. 2-4 1985.
- Matter, A., P. Homewood, C. Caron, J. van Stuijvenberg, M. Weidmann, and W. Winkler, Flysch and molasse of western and central Switzerland, in: *Geology of Switzerland, a Guide Book*, edited by R. Trümpy, pp. 261-293, Wepf, Basel, 1980.
- McNutt, M.K., M. Diament and M.G. Kogan, Variations of elastic plate thickness at continental thrust belts, *J. Geophys. Res.*, 93, 8825-8838, 1988.
- Moretti, I. and D.L. Turcotte, A model for erosion, sedimentation and flexure with respect to New Caledonia, *J. Geodyn.* 3, 155-168, 1985.
- Naef, H., P. Diebold and S. Schlanke, Sedimentation und Tektonik im Tertiär der Nordschweiz, *Tech. Ber. Nagra*, 85 -14, 147 pp., 1985.
- Ori, G.G. and P.F. Friend, Sedimentary basins, formed and carried piggy-back on active thrust sheets, *Geology*, 12, 475-478, 1984.
- Pfiffner, O.A., Fold and thrust tectonics in the Helvetic nappes (eastern Switzerland), in *Thrust and Nappe Tectonics*, edited by K. R. McClay and N. J. Price, *Geol. Soc. Spec. Publ. London*, 9, 319-327, 1981.
- Pfiffner, O.A., Evolution of the North Alpine Foreland Basin in the central Alps, in *Foreland Basins*, edited by P.A. Allen and P. Homewood, *Int. Assoc. Sedimentol., Spec. Publ.*, 8, 219-228, 1986.
- Pfiffner, O.A., W. Frei, H. Finckh and P. Valasek, Deep seismic reflection profiling in the Swiss Alps: Explosion seismology results for line NFP 20-EAST, *Geology*, 16, 987-990, 1988.
- Pinet, P. and M. Souriau, Continental erosion and large-scale relief, *Tectonics*, 7(3), 563-582, 1988.

- Tanner, H., Beitrag zur Geologie der Molasse zwischen Ricken und Hörnli, *Min. Geol. Inst. Eidg. Tech. Hochsch. Univ. Zurich, C122*, 108 pp., 1944.
- Triumpy, R., The timing of orogenic events in the central Alps, in *Gravity and Tectonics*, edited by K.A. DeJong and R. Schoffen, pp. 229-251, John Wiley, New York, 1973.
- Triumpy, R., *Geology of Switzerland, a Guide Book*, Farr York, 1973.
- A: *An Outline of the Geology of Switzerland*, 104 pp., Wepf, Basel, 1980.
- Vail, P.R., R.M. Mitchum, Jr., R.G. Todd, J.M. Widmier, S. Thompson III, J.B. Sangree, J.N. Bubb and W.G. Hatfield, Seismic stratigraphy and global changes in sea-level, in *Seismic Stratigraphy - Applications to Hydrocarbon Exploration*, edited by C.E. Payton, *Mem. Am. Assoc. Pet. Geol.*, 26, 49-212, 1977.
- Vening-Meinesz, F.A., Gravity over the Hawaiian Archipelago and over the Madeira area, *Proc. Netherlands Acad. Wetensia*, 44 pp., 1941.
- Vollmayr, v-T. and A. Wenzl, Die erdgasbohrung Entlebuch I, ein 10-tägiger Ausflug am Alpenvorland, *Bull. Ver. Schweiz. Pet. Geol. Ing.*, 53(125), 67-79, 1987.
- Watts, A.B., An analysis of isostasy in the world's oceans, I, Hawaiian-Empire sea-mount chain, *J. Geophys. Res.*, 83, 5989-6004, 1978.
- Watts, A.B. and J.R. Cochran, Gravity anomalies and flexure of the lithosphere along the Hawaiian-Empire seamount chain, *Geophys. J. R. Astron. Soc.*, 38, 119-141, 1974.
- Watts, A.B. and M. Talwani, Gravity anomalies seaward of deep sea trenches and their tectonic implications, *Geophys. J. R. Astron. Soc.*, 36, 57-90, 1974.
- Watts, A.B., J.H. Bodine and N. M. Ribe, Observations of flexure and the geological evolution of the Pacific Ocean basin, *Nature*, 283, 532-537, 1980.
- Wegmann, R., Zur Geologie der Flyschgebete südlich Elm, *Min. Geol. Inst. Eidg. Tech. Hochsch. Univ. Zurich, C176*, 256 pp., 1961.
- Willes, S.D., D.S. Chapman and H.J. Neugebauer, A thermo-mechanical model of continental lithosphere, *Nature*, 314, 520-523, 1985.
- P.A. Allen and A.B. Watts, Department of Earth Sciences, Oxford University, Parks Road, Oxford OX1 3PR, England
- B.J. Coakley, Lamont-Doherty Geological Observatory and Department of Geological Sciences, Columbia University, Palisades New York 10964.
- H.D. Sinclair, Department of Geological Sciences, Science Laboratories, South Road, Durham DH1 3LE England.
- (Received December 16, 1989; accepted November 14, 1990)
- Platt, J.P., Dynamics of orogenic wedges and the uplift of high-pressure metamorphic rocks, *Geol. Soc. Am. Bull.*, 97, 1037-1054, 1986.
- Price, R.A., Large scale gravitational flow of supracrustal rocks, Southern Canadian Rockies, in *Gravity and Tectonics*, edited by K.A. De Jong and K. Schoffen, pp. 491-502, John Wiley, New York, 1973.
- Quinlan, G.M. and C. Beaumont, Appalachian thrusting, lithospheric flexure, and the Paleozoic stratigraphy of the eastern interior of North America, *Can. J. Earth Sci.*, 21, 973-996, 1984.
- Rigassi, D., Subdivision et datation de la Molasse d'au douce inférieure du Plateau Suisse, *Palaeolab News*, vol. 1, Terraux du Temple, Geneva, 1977.
- Roache, P.J., *Computational Fluid Dynamics*, 446 pp., Hermosa, Albuquerque, N.M., 1982.
- Royden, L., E. Patacca and P. Scandone, Segmentation and configuration of subducted lithosphere in Italy: An important control on thrust-belt and foredeep basin evolution, *Geology*, 15, 714-717, 1987.
- Ruefli, W.H., Stratigraphie und Tektonik eingeschlossenen Glarner Flysches im Weissenauental (St. Gallen Oberland), *Min. Geol. Inst. Eidg. Tech. Hochsch. Univ. Zurich, C175*, 194 pp., 1959.
- Rybach, L., Geothermic and radiometric investigations, *Schweiz. Mineral. Petrogr. Mitt.*, 59, 141-148, 1979.
- Siegenthaler, C., Die Nordhelvetischen Flysch-gruppe im Semfial (Kt. Glarus), Ph.D. thesis, 83 pp., Univ. of Zurich, Zurich, 1974.
- Sinclair, H.D., The North Helvetic Flysch of E. Switzerland: Foreland basin architecture and modelling, D.Phil. thesis, Univ. of Oxford, Oxford, England, 1989.
- Sinclair, M.S. and A.B. Watts, Subidence history and tectonic evolution of Atlantic type continental margins, in *Dynamics of Passive Margins, Geodyn. Ser.*, vol. 6, edited by R.A. Scrutton, pp. 184-196, AGU, Washington, D.C., 1981.
- Sieckler, M.S., A.B. Watts and A.J. Thorne, Subidence and basin modelling at the U.S. Atlantic Passive margin, in *The Atlantic Continental Margin: U.S. The Geology of North America* vol. 1-2, edited by R.A. Sheridan and J.A. Crow, pp. 399-416, Geological Society of America, Boulder, Colo., 1988.
- Stockmal, G.S., C. Beaumont and R. Bouillier, Geodynamic models of convergent margin tectonics: Transition from rifted margin to overthrust belt and consequences for foreland basin development, *AAPG Bull.*, 70, 853-868, 1986.
- Styger, G.A., Bau und Stratigraphie der Nordhelvetischen Terlarbildungen in der Haussstock- und westlichen Karpf-gruppe, *Min. Geol. Inst. Eidg. Tech. Hochsch. Univ. Zurich, C177*, 151 pp., 1961.
- Tankard, A.J., On the depositional response to thrusting and lithospheric flexure: examples from the Appalachian and Rocky Mountain basins, in *Foreland Basins*, edited by P.A. Allen and P. Homewood, *Spec. Publ. Int. Assoc. Sedimentol.*, 8, 369-392, 1986.